ABSTRACT

Title of Dissertation: NANOPATTERNING OF RECOMBINANT PROTEINS AND VIRUSES USING BLOCK COPOLYMER TEMPLATES

Arthur von Wald Cresce, Doctor of Philosophy candidate, 2007

Dissertation directed by: Professor Peter Kofinas
Department of Materials Science and Engineering

The study of interfaces is important in understanding biological interactions, including cellular signaling and virus infection. This thesis is an original effort to examine the interaction between a block copolymer and both a protein and a virus. Block copolymers intrinsically form nanometer-scale structures over large areas without expensive processing, making them ideal for the synthesis of the nanopatterned surfaces used in this study. The geometry of these nanostructures can be easily tuned for different applications by altering the block ratio and composition of the block copolymer. Block copolymers can be used for controlled uptake of metal ions, where one block selectively binds metal ions while the other does not. 5-norbornene-2,3-dicarboxylic acid is synthesized through ring-opening metathesis polymerization. It formed spherical domains with spheres

approximately 30 nm in diameter, and these spheres were then subsequently loaded with nickel ion. This norbornene block copolymer was tested for its ability to bind histidine-tagged green fluorescent protein (hisGFP), and it was found that the nickel-loaded copolymer was able to retain hisGFP through chelation between the histidine tag and the metal-containing portions of the copolymer surface. Poly(styrene-*b*-4-vinylpyridine) (PS/P4VP) was also loaded with nickel, forming a cylindrical microstructure. The binding of *Tobacco mosaic virus* and *Tobacco necrosis virus* was tested through Tween 20 detergent washes. Electron microscopy allowed for observation of both block copolymer nanostructures and virus particles. Results showed that Tween washes could not remove bound Tobacco mosaic virus from the surface of PS/P4VP. It was also seen that The size and tunability of block copolymers and the lack of processing needed to attain different structures makes them attractive for many applications, including microfluidic devices, surfaces to influence cellular signaling and growth, and as a nanopatterning surface for organized adhesion.

NANOPATTERNING OF RECOMBINANT PROTEINS AND VIRUSES USING BLOCK COPOLYMER TEMPLATES

by

Arthur von Wald Cresce

Dissertation proposal submitted to the Faculty of the Graduate School of the
University of Maryland at College Park in partial fulfillment
of the requirements for the degree of
Doctor of Philosophy
2007

Advisory Committee:

Professor Peter Kofinas, Chairman/Advisor
Professor William E. Bentley
Professor Robert M. Briber
Professor James N. Culver
Professor Mohammad Al-Sheikhly

DEDICATION

To my grandfather, Dominic Santin Toffolo.

His was the joy of science.

ACKNOWLEDGEMENTS

Without being surrounded by my friends and family, this research would not have been possible. I must first express my infinite gratitude to my advisor, Peter Kofinas, for his endless patience and good spirits. He was a constant presence with expert advice and motivation, and he always seemed to know when to alleviate a difficult day with a funny e-mail or a trip for espresso. "*Enjoy, my friend!*" His guidance allowed me to learn about the many nuances of good scientific work. I take away a lifetime of experience from my time as a graduate student in his laboratory group.

My family was a constant inspiration to me. My father, Arthur R. Cresce Jr., and my mother, Mary Elizabeth Toffolo-Cresce, both have survived monumental academic labor. They were always able to motivate and lift me in difficult times, as well as celebrate my successes. My brother Vince and sisters Nicole and Lisa were always support-

ive of my work, and had faith in me through the whole of graduate school.

My grandparents, Dorothy Toffolo, Arthur Cresce Sr., and Anita Cresce were all able to provide me with sage advice and wisdom, and none of them ever tired of hearing about my research. Their loving support and good food nourished me during graduate school.

My labmates became my close freinds, and their expertise and humor made laboratory life enjoyable and delightfully unpredictable. Linden Bolisay, Dan Janiak, Ayan Ghosh, Ta-I Yang, Angela Fu, Brendan Casey, and Sanem Argin were all part of my research group, and each contributed to my project in their own unique way. I'm not sure what I would have done without the constant advice and criticism of Linden, Dan, and Ayan, who contributed more to my project than I think they realize. Thanks to Linden for giving me the tobacco viruses that he spent hours to culture and purify, and for perpetually finding humor in our work. I owe Dan for all his advice as well as the times that he put up with my shenanigans. Special thanks goes to Ayan for bringing home the cricket bat of Kashmir willow, which helped me fend off questions during my proposal. I will miss the jokes, the many, many quotes, and the constant peanut gallery that was our office. I also thank Nicolae Albu for everything I learned from

our many discussions, especially those that had nothing to do with science.

The undergraduate students in our lab helped me to grow as an advisor, even as they proved they were more than capable to work in a professional laboratory. My thanks to Josh Silverstein, Rachel Emmel, Sam Lopez, Wahab Jilani and Matt Getz.

I am extremely grateful to Angela Lewandoski and Dr. William Bentley, who so generously provided the proteins and advice that made this project possible.

I also owe thanks to Robert Briber and his research group. Although Dr. Briber occasionally tried to sidetrack me with gorgeous British car magazines filled with Aston Martins, BMWs, and Lamborghinis, he provided constantly helpful suggestions and expertise that helped shape my project. His students, Wonjoo Lee, Xin Zhang, Zhaoliang Lin, Chris Metting, and Sangcheol Kim, treated me as part of their group and never failed to assist me. They showed me what it means to collaborate between groups.

I must also thank Steve Bullock, Sufi Ahmed, Pinar Akcora, and Maria Crassas, all of whom graduated from the Kofinas group before me. They were my mentors, and I use their techniques and strategies to this day. Their expertise and abilities were world-class, and I

tell stories of each of them when I must explain how I know things. They helped form me when I was a fresh, unsuspecting new graduate student. The lab was not the same without them.

I thank Alan Jaworski for helping to build my physical strength as well as my mental strength. I will never forget flipping the 800 pound tire on those cold mornings not for fun, but as a workout. I thank my friends Mike Flint, Brett Neuberger, and Greg Oberson, whose friendship and advice kept me constantly on my toes.

I especially thank my many friends whose constant humor and support made me laugh even in the most difficult times. Thanks to Kevin Knupp and our many academic competitions. The pursuit of excellence we began in high school has come to fruition here in graduate school. My gratitute goes to Eric Arnold, Mike Urban, Greg Vogt, Meghan Fannin, Keon Burley, Mike and Meghan Phelan, Chris Boccanfuso, Chris Hamilton, John Albert, James Woody, and all the other people I am so very lucky to consider freinds. I couldn't have done it without you guys. I only hope that someday I can provide the support and humor that you all provided me.

TABLE OF CONTENTS

LIST OF FIGURES

Chapter 1

Introduction

1.1 Motivation

This thesis is an investigation into the interaction between a block copolymer surface and both a virus and a protein. Examination of the interface between biological and inorganic systems is rapidly expanding, as many events characteristic of biological systems occur at, or are initiated on, surfaces and boundaries. Traditional materials solutions to bio/synthetic interfaces have relied on micropatterned surfaces created through lithography or other structured deposition methods. Nanoscale structures will be created by block copolymer microphase separation. These block copolymer surfaces are examined for their ability to pattern both a protein and a virus. A norbornene-based block copolymer is synthesized and its success in retaining and patterning a modified green fluorescent protein is determined. A polystyrene-*b*-poly(4-vinylpyridine) copolymer surface

is examined for its ability to bind two different plant viruses, *Tobacco mosaic virus* and *Tobacco necrosis virus*. It is hoped that this research will enhance the understanding of the interaction between an inorganic surface and biological species such as viruses and proteins.

1.2 Significance and application

There is much practical significance that can be taken from this project. Research into the use of block copolymers as nanopatterning surfaces for viruses does not yet exist. This study is unique in its use of a block copolymer template for the creation of regularly-shaped metal loaded domains for the purpose of interacting with biological species such as proteins and viruses. Block copolymers present a unique advantage in that they inherently form regular domains of nanometer size. Control over domain morphology can be exerted through simple choice of block length and composition, allowing a wide range of available structures and functional groups. These block copolymer patterns are valuable in that they can achieve nano-scale patterning of target species that is similar to the patterning of the block copolymer surface itself.

A norbornene copolymer has been synthesized that can selectively bind histidine-tagged green fluorescent protein (his_6GFP). his_6GFP is a genetically modified protein, created through recombinant DNA synthesis, which contains a residue of six histidine amino acids (his_6) at the amino terminus of green fluorescent

protein [1]. This tag is commonly used as a purification tool, as the histidine tag chelates with metal ions, allowing it to be separated from other accompanying proteins [2]. The copolymer surface, functioning as a (his_6)-tagged protein chelator, could serve as an advanced, organized surface for protein separation. It would allow for the binding, detection, and analysis of proteins that are tagged. In the future, the same block copolymer surface could be decorated with ordered arrays of antibodies, rather than metal-containing domains, allowing for even greater specificity and opening the range of applications from tagged proteins to virtually any nano- or microscopic species. Systems which use inorganic surface-bound antibodies as biosensors are already beginning to appear in literature [3, 4, 5]. A block copolymer surface could therefore be integrated into a detection system designed to identify and quantify biological molecules and other larger entities. Nanopatterning of protein particles could allow for greater ease and speed in structural studies of proteins, especially x-ray crystallography which relies on protein crystals to derive structural data.

Applications also exist for viruses that are nanopatterned by the polystyrene-*b*-poly(4-vinylpyridine) block copolymer. For example, nanopatterned arrays of viruses on a block copolymer surface could aid X-ray analysis-based solutions to the surface structure of viruses. Ordered immobilization of virus particles on a nanopatterning surface could eventually address the difficulty of preparing virus particles for X-ray analysis. Information about virus geometry and even viral

surface electron density can be determined from X-ray scattering data [6].

Research has shown that nanotextured surfaces can influence the behavior of viruses and cells [7]. Because much of the chemistry involved in signaling and recognition in biology involves surface interactions [8, 9], having a tunable surface that can be altered to study different organisms or to elicit different reactions could be quite valuable as a research tool.

Microfluidic devices are devices that deal with fluids on a very small volume scale, often on the order of nanoliters. These devices are receiving much research attention and are becoming more commercially viable, especially as a microbatch tool to reduce experimental costs. Several companies, including Hewlett-Packard, Agilent Technologies, and Caliper Technologies, are producing working production versions of lab-on-a-chip devices, an example of which is seen in Figure 1.1. Often, as in the case of the Agilent 2100 bioanalyzers, they are used for electrophoretic analysis of DNA, RNA, and proteins. The 2100 can be seen in Figure 1.2. Even NASA has invested significant research in microfluidic devices, as it plans to include such devices in the Modular Assays for Solar System Exploration (MASSE) project, scheduled to start in 2013, where the microfluidic chips will help to detect possible bacteria and life forms on other planets. A nanopatterned block copolymer surface seems a natural fit for such a microfluidic system, as its ease in processing should allow it to be integrated, especially in the capacity of binding studies, species detection, or structural characterization.

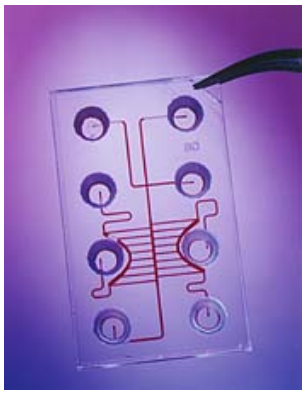

Figure 1.1: Picture of the lab-on-a-chip device being developed by Agilent Technologies.

Figure 1.2: Agilent Technologies 2100 LabChip used for DNA, RNA, and protein analysis through electrophoresis.

A surface capable of nanopatterning a protein, or any biological molecule, could also be considered as a patterned substrate used to underpin a molecular computation device. Molecular computation devices and DNA computing systems are slowly developing, but show the promise of being able to perform feats of calculation that are beyond traditional solid-state processors [12, 13].

1.3 Biointerfaces

Biologically active materials systems have become a popular topic for research in the past two decades. The application of materials science in biology is quite diverse [14, 15, 16, 17, 18, 19, 20, 21, 22, 23, 24, 25]. An important area of interest in this growing field is the study of the interface between inorganic and biological systems.

In their natural state, biological systems display a remarkable ability to recognize, sort, and act on information relayed through different chemical signals and environmental conditions. As recently as 2001, efforts have been made to emulate the versatility of biological surface interfaces [26, 27, 28, 29, 30]. For example, silicon-based micropatterned surfaces have been made that are able to direct the growth of retinal cell neurite growth [31].

Much of the current research on this topic of biological-inorganic surface interfaces involves patterning that exists on the microscale. Lithographic techniques can produce a wide variety of structures, such as arrays of lines and dots [32], that have been proven to affect the direction of growth of cells, the adhesion of cells to a substrate, and the shape and health of cells attached to the substrate [85]. Rather than using lithography to pattern an inorganic surface, block copolymers were employed to create a surface decorated with nanometer-sized structures.

1.4 Block copolymers

Block copolymers are polymer molecules that contain two or more unlike homopolymers that are chemically linked to form a single polymer chain. Usually, homopolymers are insoluble in one another, and often form two phase systems at equilibrium. Block copolymers are physically limited in their ability to phase separate, because the blocks are linked together by a covalent bond. Therefore, in order to reach a state of lowest free energy, a block copolymer system with sufficiently high homopolymer block incompatibility will "microphase separate" into structures that seek to minimize contact between the two homopolymer blocks. This process of microphase separation results in periodic structure of nanometer-sized domains rich in one block or the other.

The physical limitation of block copolymers means that the traditional expression of free energy of mixing should be modified in order to better describe the separation process. The Gibbs free energy of mixing is expressed as:

$$\Delta G_m = \Delta H_m - T\Delta S_m \tag{1.1}$$

where ΔG_m is the Gibbs free energy of mixing, ΔH_m is the enthalpy of mixing, and ΔS_m the entropy of mixing. Negative values of ΔG_m indicate conditions favorable to mixing, while positive values of ΔG_m indicate instability leading to phase separation.

From the theory developed by Flory and Huggins [39], it can be written that:

$$\Delta G_m = RT\left[n_1 \ln \phi_1 + n_2 \ln \phi_2 - n_1 \phi_2 \chi_{12}\right] \tag{1.2}$$

The Flory-Huggins interaction parameter χ was introduced to account for the energy of interspersing polymer and solvent molecules [39, 40]. In 1980, Ludwik Leibler further modified the Flory-Huggins χ parameter to include the enthalpic effect of non-bonded interactions present in block copolymer systems [34]. Leibler's modified expression of χ was as follows:

$$\chi = \frac{1}{k_b T} \cdot \left[E_{ab} - \frac{(E_{aa} + E_{bb})}{2}\right] \tag{1.3}$$

where E_{ij} refer to the contact energy between components i and j, k_b is Boltzmann's constant, and T is temperature.

According to this theory, χ is negative and favors a and b component mixing when E_{ab} is larger than the sum of E_{aa} and E_{bb}, meaning that lower energy in the system is achieved by having more a-b contacts than a-a or b-b contacts. A positive χ occurs when E_{ab} is less than the sum of E_{aa} and E_{bb}, and the system prefers homogeneous contacts. In block copolymers with components A and B, Leibler noted that the repulsion between blocks A and B were strong even when the repulsion between monomers A and B were fairly weak [34].

In a block copolymer with block components A and B, instability between the blocks tends to result in a positive χ and favors homogeneous contacts, thus resulting in phase separation. Because of their physical limitation in separating,

a system of microdomains results from this process of phase separation. These microdomains, as Leibler noted, are not always random and often form structures with a regular arrangement. In a diblock copolymer consisting of two different blocks, the structures caused by microphase separation are observed in four major groups - spheres or cylinders of one block in a matrix of the other block, a gyroidal or interconnected structure, and alternating lamelle of each block. A diagram of each of these states is seen in Figure 1.3. Leibler deduced that the two most important factors governing the formation and geometry of these microphases were the composition f, the fraction of monomers A in the block copolymer chain, and the product χN, where χ is the Flory-Huggins interaction parameter and N is the degree of polymerization. The parameters f and χN can be used to construct a phase diagram showing the regions of stability of the different phases with respect to the degree of polymerization f and the block fraction N. This phase diagram is seen in Figure 1.4.

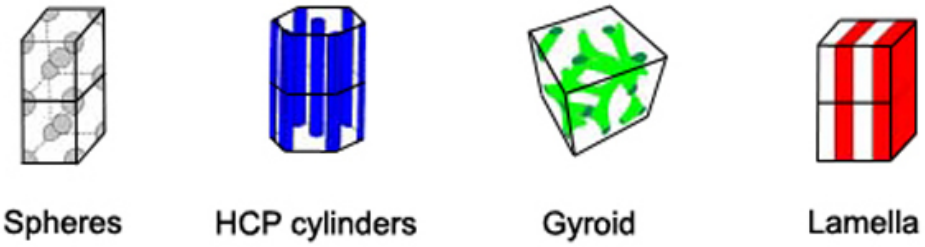

Figure 1.3: Schematic of the four major morphologies observed in a diblock copolymer.

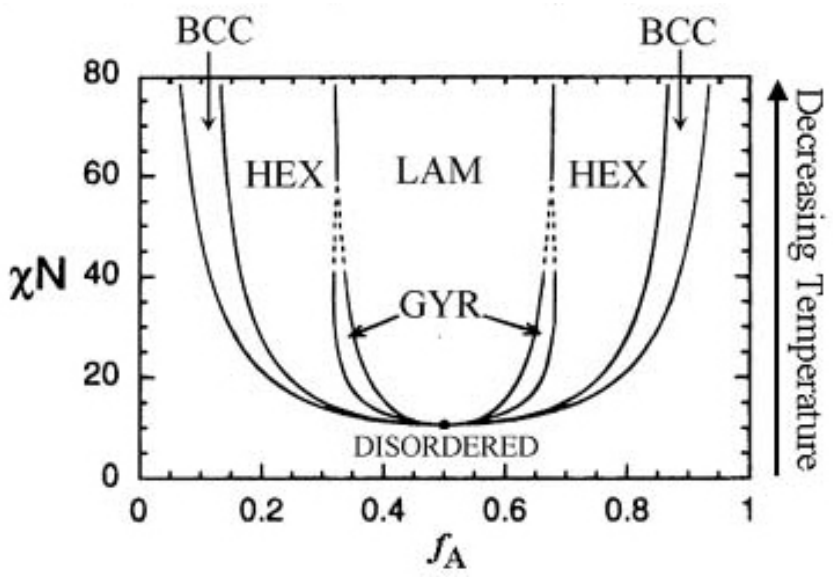

Figure 1.4: Mean-field phase diagram of a diblock copolymer, showing the variation in morphology with change in volume fraction f of block A and the product of the Flory interaction parameter χ and degree of polymerization N. Adapted from Matsen and Bates 1996 [38].

Block copolymers represent a unique opportunity to design and engineer nanometer-sized structures. The synthesis of quantum dots, for example, requires the use of capital-intensive techniques: either one must use lithographic masks and material deposition techniques like metal-organic chemical vapor deposition or molecular beam epitaxy, or one must take advantage of frustrated interactions between a substrate and a slightly lattice-mismatched epitaxial film layer [44]. Block copolymers form equilibrium nanostructures that do not require such external synthetic techniques, but rather take advantage of the natural process of

microphase separation inherent in block copolymers.

1.5 Targeted metal loading of single blocks in a block copolymer

In a block copolymer, single blocks can be chosen so that they have the chemical ability to take up metal ions. Robert E. Cohen performed significant work showing the ability of a norbornene-based block copolymer to take up metal ions leading to the formation of templated metal nanoclusters [46, 47, 48, 49, 63]. In this thesis, two block copolymers will be examined for their nanopatterning ability: norbornene-*b*-5-norbornene-2,3-dicarboxylic acid and polystyrene-*b*-poly(4-vinylpyridine). Both of these copolymers contain a block that is inert to metal ions, norbornene and polystyrene. The second block in both these copolymers is able to complex metal ions through complexation [41, 42, 43, 46, 47, 48, 49].

In these two copolymers, metal loading occurs through metal ion sequestration in the receptive block. The dual carboxylic acid arms of 5-norbornene-2,3-dicarboxylic acid provide pendant oxidation sites that serve to immobilize and stabilize passing metal ions [46, 47, 49]. In polystyrene-*b*-poly(4-vinylpyridine), the pendant 4-vinylpyridine nitrogen with its unshared electron pair allows metal complexation into the poly(4-vinylpyridine) block. There are several methods of introducing metal ions into the microstructure of a block copolymer. Metal-

loaded polymer systems have been synthesized by deposition of metal vapor into liquid monomer followed by polymerization, deposition of metal ions into polymer films from supercritical CO_2 [45], and exposure of block copolymer to metal salts to polymers both as solid films and when in solution with the copolymers.

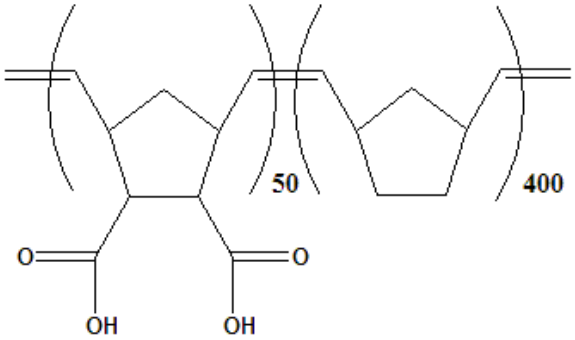

Figure 1.5: Structure of norbornene-*b*-5-norbornene-2,3-dicarboxylic acid.

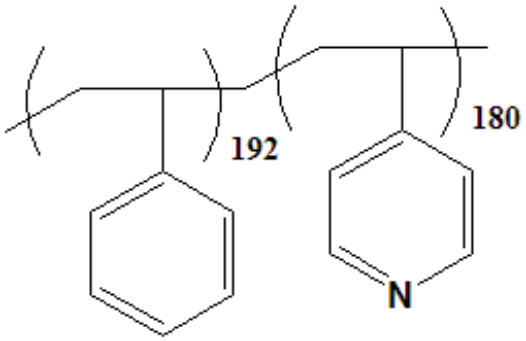

Figure 1.6: Structure of polystyrene-*b*-poly(4-vinylpyridine).

In this study, both block copolymers will be exposed to metal salts while in solution. Initial success in using nickel as a chelating agent toward histidine-tagged green fluorescent protein led to the use of nickel in both protein and virus binding experiments. Exposure to the copolymer in solution results in high specificity in

targeting the nickel ion to the receptive block of each block copolymer. Electron micrographs showed that nanoparticle formation is not observed. Rather, the receptive block complexes the metal generally over its domain with apparently minimal leakage between blocks.

The issue of metal leakage between the blocks is addressed by selecting polymers that possess glassy blocks, i.e. the polymer at the experimental temperature is below its glass transition temperature. The diffusion constant of species dispersed in a glassy copolymer is low, often ranging as low as 10^{-16} to 10^{-18} cm^2/sec [50, 51]. Because of the diffusion barrier between the two blocks in both copolymers, the metal ions are not observed to diffuse into the inert block. Electron microscopy was the primary method of analysis in this thesis. Leakage of metal ions, visible as contrast in the electron microscope, was not observed in either polynorbornene or polystyrene.

In this study, the block copolymers studied will be used to uptake metal ions to form templated metal-containing microstructure. The metal ions used, especially nickel, show affinity toward certain functional groups, and are valuable as complexed ions. Nickel is often used as the basis for chelation-based protein separation systems, and there are numerous commercial examples of immobilized metal-affinity chromatography (IMAC) systems available to researchers today.

In order to test the hypothesis of protein and virus nanopatterning, this project will show that the surface of a metal-functionalized amphiphilic block

copolymer is capable of chelating both proteins and viruses. By doing so, it will be demonstrated that such a copolymer surface can form the basis of devices intended for the purification, identification, and analysis of proteins and viruses.

1.5.1 Ring-opening metathesis polymerization

Ring-opening metathesis polymerization (ROMP) was utilized to form the norbornene/norbornene dicarboxylic acid (which will be subsequently referred to as NOR/NORCOOH) diblock copolymer [52]. ROMP is a powerful synthetic tool that can be used to form block copolymers with various functional groups [54] and low polydispersity. Ring-opening metathesis is a specific type of metathesis polymerization where a strained cyclic olefin monomer switches alkenic ($R_2C{=}CR_2$) ligands with an initiator [55, 56]. A mechanism of the process of ROMP is seen in 1.7.

Metallocene-initiated ROMP is a living chain polymerization that proceeds with initiation and propagation, and has no natural termination reaction. Therefore, a ROMP system will consume all monomer in a reaction and retain its polymerization activity. If a different ROMP-capable monomer is added, the polymerization will continue and will form a block copolymer. Ethyl vinyl ether is used to artificially terminate the ROMP reaction used here to create NOR/NORCOOH. Ethyl vinyl ether complexes with the active catalyst, but does not undergo ROMP, so it effectively kills the polymerization.

Various catalysts have been devised since the introduction of the metal-carbene induced ROMP of cyclic alkenes, using ruthenium, molybdenum, and titanium [53, 55, 56]. The introduction of metallocene catalysts by both Grubbs [58] and Schrock [57] allowed the formation of metathesis polymers with low polydispersity. Robert H. Grubbs is well known for his contributions to metathesis polymerization, and specifically to the development of the effective ruthenium based ROMP catalyst [1,3-Bis-(2,4,6-trimethylphenyl)-2-imidazolidinylidene) dichloro (phenylmethylene) (tricyclohexyl-phosphine) ruthenium], known as Grubbs's second generation catalyst [53, 52, 54]. This second generation benzylidine imidazole version of Grubbs's ruthenium ROMP catalyst was used to initate polymerization of the NOR/NORCOOH copolymer used in this study [59]. Its structure is seen in Figure 1.8.

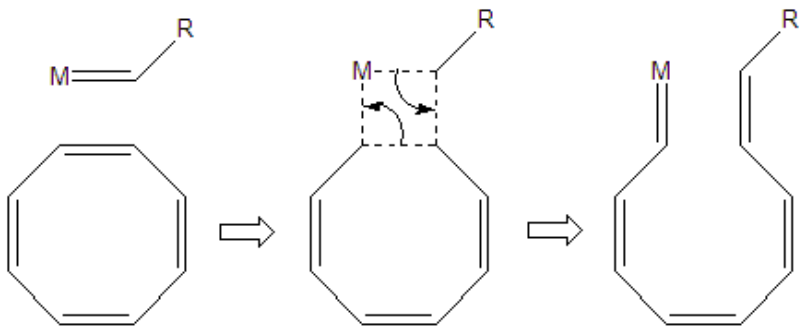

Figure 1.7: Mechanism of ROMP. The metal-carbene ligand of the ROMP initiator metathesizes the strained double bond of a cyclic monomer. The formation of a metallocyclobutene intermediate species leads to the ROMP product with monomer and initiator ligands switched.

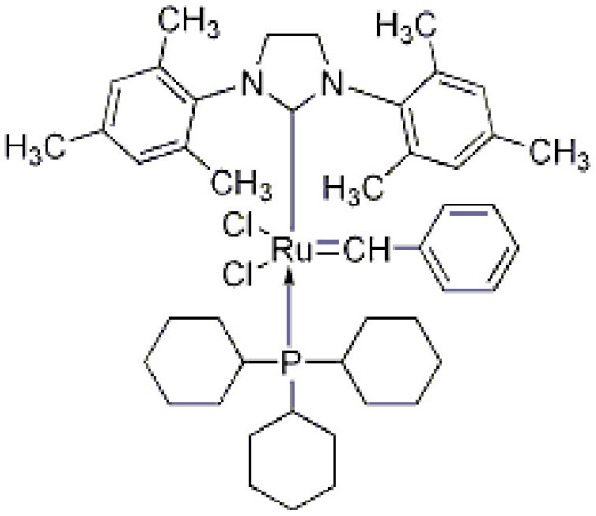

:

Figure 1.8: Grubbs's second generation ROMP initiator [1,3-Bis-(2,4,6-trimethylphenyl)-2-imidazolidinylidene) dichloro (phenylmethylene) (tricyclohexyl-phosphine) ruthenium].

Chapter 2

Nanopatterning of Recombinant Proteins Using A Norbornene Block Copolymer Template

2.1 Motivation

Here, a norbornene block copolymer will be discussed that is capable of selectively binding histidine affinity tag modified green fluorescent protein. There are several possible commercial applications of such a system. For example, there has been increasing amounts of research in microfluidic devices and the idea of lab-on-a-chip technology, and an ordered polymer surface may aid in the production of arrays of single nanoreactors in microfluidic devices. This could function in applications including combinatorial chemistry for drug discovery and high throughput analysis in genomics and proteomics. Nanocale confinement studies depend on the development of appropriate nanoscale patterns such as those present by the self-assembly of block copolymers. The polymer surface, function-

ing as a hexahistidine (his_6)-tagged protein chelator, could serve as the basis for a fast protein separation device in the process of protein purification.

2.2 Introduction

The ability to immobilize proteins on nanometer sized patterns has become a major challenge for the development of bioengineered surfaces. Nanopatterned surfaces are known to influence cell function through surface-triggered interactions [64]. The ability to vary the topology and separation between nanopatterned recombinant proteins on the surface of a block copolymer may lead to the construction of devices that can examine cellular signaling. In addition, the ability to spatially control the immobilization of small amounts of recombinant proteins may provide better platforms for the study of single molecular events, such as through AFM force measurements.

This study examines the ability of the diblock copolymer surface to selectively bind hisGFP. Kumar and Hahm demonstrated the feasability of this system in a recently published study [65]. In order to accomplish specific protein adsorption to a block copolymer surface, a norbornene block copolymer was first loaded with different metal ions in order to determine the most effective ion to use in the protein binding system. Copper [66], iron [67], and nickel [68] ions are mentioned in literature as being effective in chelating histidine-tagged proteins. Currently, nickel chelation columns are used regularly to separate histidine-tagged

proteins from a mixture in order to isolate the tagged protein [69] in a process first introduced by Porath *et al.* [70].

Monomers of norbornene and norbornene dicarboxylic acid were copolymerized together to produce an amphiphilic diblock copolymer. The hydrophilic block of these copolymers were used to template the formation of metal nanoparticles. Robert Cohen developed a method where the carboxylic acid block of a diblock copolymer was used to template the formation of nickel nanoparticles within the hydrophilic blocks of these copolymers [46, 49]. While this metal-templating technique has been successful in the methyltetradodecene-norbornene dicarboxylic acid system, the same principle holds for the polymer systems used in this experiment, and was verified in this study through electron microscopy. Ring-opening metathesis polymerization (ROMP) was chosen to form the norbornene-*b*-5-norbornene-2,3-dicarboxylic acid (NOR/NORCOOH) diblock copolymer [53, 52, 54, 59].

The protein species used is a modified version of green fluorescent protein (GFP). A hexahistidine (his_6) affinity tag is grafted to the N' terminus of the GFP through the expression of recombinantly modified DNA [60, 1]. The structure of his_6-tagged GFP can be seen in Figure 2.1. This histidine tag has a strong affinity for metal ions, with which it forms stable complexes [61]. Studies have shown that the histidine tag does not affect the structure and function of GFP, so that the standard methods of analyzing for GFP can also be used with hisGFP.

Binding of the hisGFP to the surface can thus be connected to the detection and intensity of fluorescence coming from a film exposed to hisGFP.

Figure 2.1: Schematic structure of his_6GFP. The protein forms a cylindrical, can-like structure surrounding a fluorescent chromaphore. The his_6 tag is seen as the tail on the lower right of the main protein structure.

Once the nickel ion was selected from the three metals being tested, the actual method of protein binding was investigated. Specifically, it must be known whether it is the his_6 tag on the protein that is responsible for binding, or whether other functional groups present on the protein can interact with and bind to the metal groups on the copolymer surface. In order to separate these two effects, the

binding of hisGFP was compared directly to that of untagged GFP. In addition, it must be established the metal nanoclusters in the copolymer are responsible for binding hisGFP. Therefore, the experiment must also eliminate the possibility that the norbornene copolymer itself has no affinity to the protein or to the his_6 tag. Tween 20 detergent will be used to wash weakly bound his_6GFP from the block copolymer surface. Tween 20 is a polysorbate, and it is a non-ionic surfactant that is effective at disrupting weak protein interactions, and is used both to remove peripheral proteins from membranes and is also used as a blocking agent in membrane-based immunoassays. Its structure is seen in Figure 2.2.

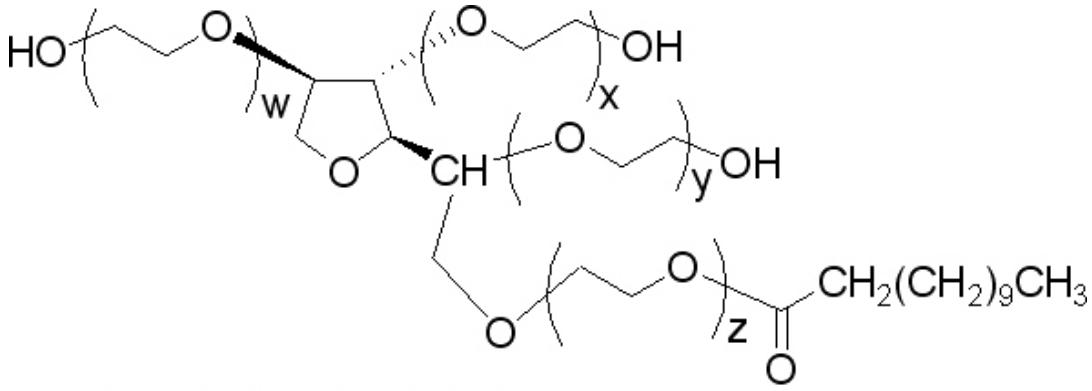

Figure 2.2: The polysorbate detergent Tween 20.

2.3 Experimental design

Green fluorescent protein (GFP) was purchased from ClonTech Laboratories, as part of the Living Colors recombinant protein line (rGFP). hisGFP was synthesized through the expression of recombinantly modified DNA and purified

according to literature procedures [1]. Tween 20 was purchased from Aldrich and diluted in deionized water. Tetrahydrofuran (THF) and norbornene (NOR) were purchased from Aldrich, distilled over sodium, and then degassed three times through a freeze/pump/thaw process. 5-norbornene-2-*endo*,3-*exo*-dicarboxylic acid (NORCOOH) was purchased from Aldrich, dried in vacuum and stored in an argon-filled MBraun LabMaster100 glovebox. Grubbs's second generation ROMP initiator [1,3-Bis-(2,4,6-trimethylphenyl)-2-imidazolidinylidene) dichloro (phenylmethylene) (tricyclohexyl-phosphine) ruthenium] was also purchased from Aldrich, stored in the glovebox, and used as recieved. All reactants were distilled and dried before use, and the polymerization took place in the glovebox. Electron microscopy was performed on a Hitachi H600AB electron microscope with accelerating voltage of 100 kV. Fluorescence testing was performed using a Perkin-Elmer LS55 Luminescence Spectrometer with excitation at 395 nm and luminescence at 508 nm [71]. Data was taken by averaging a series of ten readings into one fluorescence data value. Three films of each type were tested in order to establish experimental error and account for variations in luminescent intensity across the film surface.

2.3.1 Synthesis of protected NORCOOTMS monomer.

10 g of NORCOOH was dissolved in 400 mL dry ethyl ether and allowed to stir for 4 hours. With the NORCOOH completely dissolved, 10 mL of pyridine

and 5 mL of chlorotrimethylsiloxane were added to the stirring solution in the glovebox. Pyridine hydrochloride precipitated from the stirring ether, and this white precipitate was filtered out by pouring the reaction mixture through a 1 cm bed of Celite. The product, norbornene dicarboxylic trimethylsilyl ester (NORCOOTMS), was recovered and purified through three cycles of recrystallization in ethyl ether. The final, pure NORCOOTMS appeared as a white powder and was vacuum dried and stored in the glovebox.

2.3.2 Synthesis of NOR_{400}/$NORCOOH_{50}$ diblock copolymer.

The diblock copolymer was formed by first initiating the polymerization of the NORCOOH block. NORCOOTMS was dissolved in THF to a concentration of 1 mmol/mL. Grubbs's second generation initiator was added so that the mole ratio between initiator and NORCOOTMS was 1:50, giving a dark purple solution. The purple solution was vigorously stirred and allowed to polymerize for 24 hours. At the end of this period, the purified and dried NOR was added to the reaction mixture. NOR was dissolved in solution in THF at 0.2 mmol/mL. This reaction was allowed to continue for 6 hours, and then it was removed from the glovebox and halted with the addition of 200 μL of ethyl vinyl ether. The polymer was recovered by precipitation in a chilled mixture of 400 mL methanol, 40 mL distilled water, and 5 mL glacial acetic acid. The solid polymer obtained from

this process was white with a slight purple tint caused by trace amounts of the Grubbs catalyst, and was washed thoroughly with pentane to remove unreacted monomer. The final washed product was dried in vacuum, then redissolved in pure THF at 1 mg/mL. This mixture was used to form NOR/NORCOOH films. A schematic of this reaction process is shown in Figure 2.3.

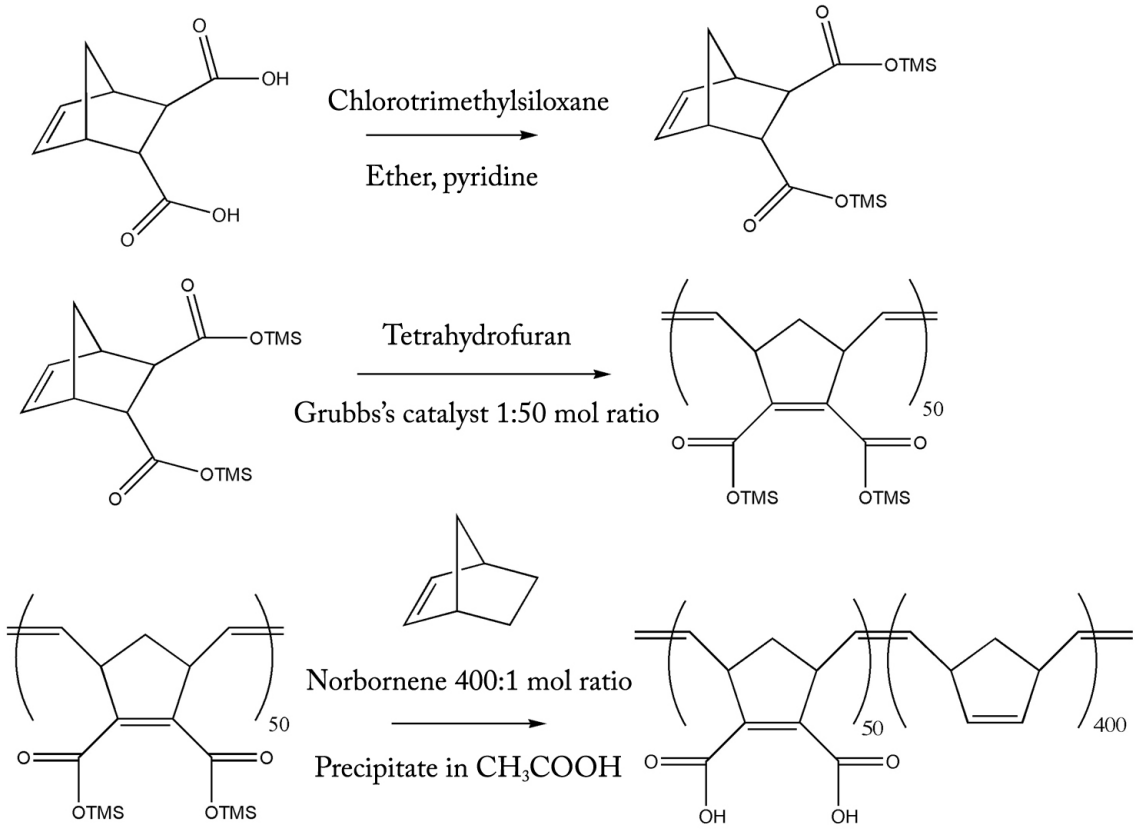

Figure 2.3: ROMP synthesis of $NOR_{400}NORCOOH_{50}$, starting with the protection of acid group with TMS, formation of the NORCOOTMS homopolymer, and block copolymerization of NOR onto the living NORCOOTMS homopolymer.

Films used for TEM study were cast from a solution of THF and 1% w/v nickel

nitrate in 5-cm diameter, flat-bottomed containers made from Bytac™ PTFE coated aluminum sheets within a THF-filled desiccator over the course of 7 days. Upon casting, the polymer films were microtomed and examined in the TEM. During this study it was found that films exposed to an aqueous metal ion solution post-casting had poor resolution in the TEM, and so solution-doped polymers were used to reveal the morphology of the copolymer. This was performed only for the TEM, and was done using nickel, which was found by Cohen in his work to bind to the -COOH containing block only in very low amounts compared to both copper and iron [46]. It was assumed that if nickel would bind in sufficient amount to allow for observation in TEM, then both copper and iron would also.

Films that were used for surface binding tests were cast on the surface of glass slides that had been stored at 120 ℃ and sterilized with alcohol and acetone. 3 mL of the polymer solution was spread evenly over the slide, forming a uniform, clear film over the slide. To prepare the NOR/NORCOOH block copolymer for protein adsorption, films of the copolymer were cast on glass slides which had been heated to 120 ℃, then washed in acetone and ethanol. Films were cast by allowing 3 mL polymer solution (at 1 mg/mL) to evaporate on the slide, giving a uniform thin film of NOR/NORCOOH on the slide. In all experiments, the proteins hisGFP and GFP were dissolved in aqueous solutions at a concentration of 1 mg/mL.

2.4 Binding study of hisGFP on NOR/NORCOOH surface with different metal ions

To test the hisGFP binding effectiveness of different ions, three metal ion species were examined: nickel, copper, and iron. NOR/NORCOOH films were soaked in solutions of metal salts to add metal ions to the surface -COOH groups. Nickel nitrate $(NiNO_3)_2$, copper sulfate hexahydrate ($CuSO_4$-$6H_20$), and iron chloride ($FeCl_3$) were dissolved in water at a concentration of 100 μg/mL. NOR/NORCOOH films were exposed to the aqueous solution for 12 hours. Three NOR/NORCOOH films were exposed to each metal type to provide experimental spread during data collection. The films were removed from the metal solution, washed with deionized water, allowed to dry for 1 hour, then exposed directly to the hisGFP solution. hisGFP exposure was limited to 10 minutes, after which the films were washed with 1 % Tween 20 detergent solution. This step was performed in order to remove all proteins not specifically bound to the metal groups on the surface of the polymer. The treated films were immediately tested in a fluorescence spectrometer to quantify the amount of protein held on the polymer surface. Baseline was established by taking the fluorescence of the empty test chamber as well as that of the blank glass slide, and the polymer both with and without metal loading. Since these values were very similar, they were averaged together to give a single baseline value to which fluorescence of bound hisGFP was compared.

2.5 Fluorescence of hisGFP on NOR/NORCOOH

Polymer films were cast and loaded with nickel ions in an identical fashion as the previous metal ion-hisGFP affinity test. Two identical film sets were cast to test the hisGFP binding directly against that of GFP without the histidine tag. This meant casting two sets of nickel-loaded block copolymer, as well as two sets of plain, non-metal containing copolymer. Two glass slides were also used, as before, to ensure the glass gives no fluorescent background readings. These test films were exposed directly to the hisGFP or GFP solution. Protein exposure was limited to 10 minutes, after which the films were washed with 1 % Tween 20 detergent solution. This step was performed to remove all proteins not specifically bound to the metal groups on the surface of the polymer. The treated films were immediately tested in a fluorescence spectrometer to quantify the amount of protein held on the polymer surface. Baseline was established by taking the fluorescence of the empty test chamber as well as that of the blank glass slide, and the block copolymer both with and without metal loading. As in the previous experiment, the empty chamber, glass slide, and polymer with and without metal gave nearly the same fluorescence value, and so were averaged together to give a single baseline value. Because there were no competing fluorescence sources in the system, it was possible to detect bound GFP fluorescence and bound hisGFP fluorescence in order to compare binding of the GFP against hisGFP.

2.6 Results and discussion

Gel permeation chromatography (GPC) was used to examine the molecular weight and polydispersity of the NOR/NORCOOH diblock copolymer produced from ROMP. It was found that the weight average molecular weight of the copolymer was within 5 % of the target (46773 g/mol) for a 400/50 block ratio, with a polydispersity index (PDI) of 1.21. Transmission electron microscopy (TEM) allowed direct observation of the copolymer's microphase separated morphology. The 400/50 NOR/NORCOOH block ratio produced spherical domains of NORCOOH with an average diameter of 30 $\pm$ 5 nm, which can be seen in Figure 2.4.

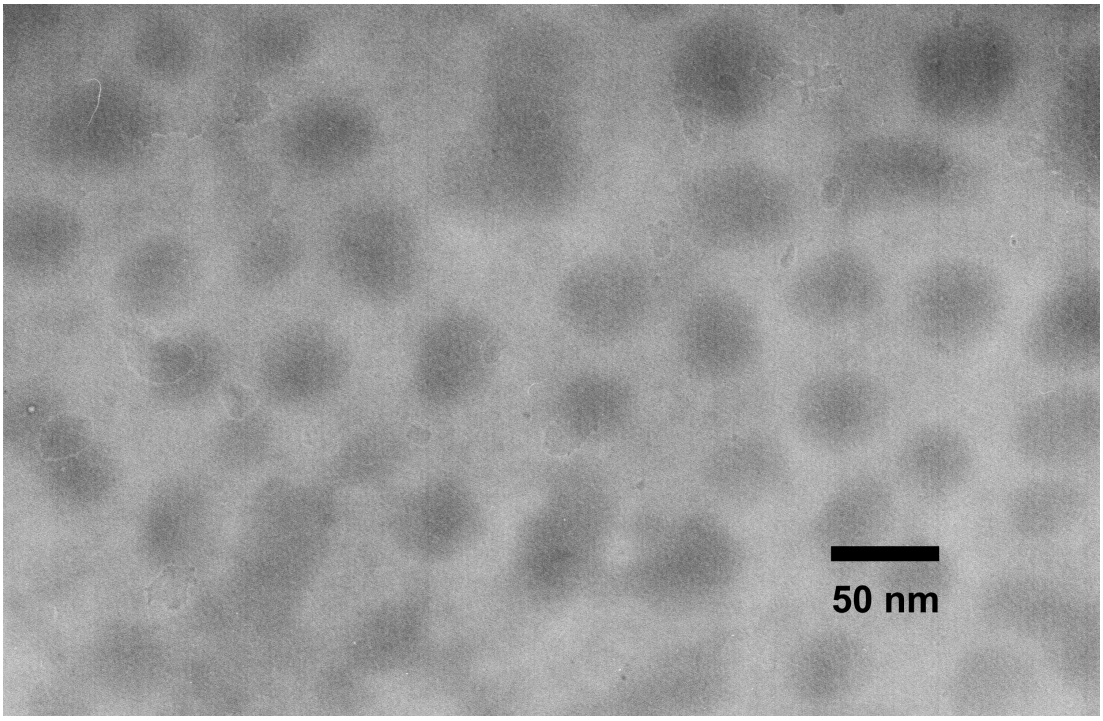

Figure 2.4: TEM micrograph of the nickel-loaded $NOR_{400}NORCOOH_{50}$ diblock copolymer.

The glass slide and polymer films that were not exposed to hisGFP achieved only baseline fluorescence, as expected. The metal-loaded films, on the other hand, showed significant fluorescence. Among the three metal ions tested in the block copolymer, nickel proved the most effective, giving a fluorescence of 70.58 $\pm$ 2.11 arbitrary intensity units. Copolymer films treated with copper and iron ions also showed hisGFP binding, but showed significantly less fluorescence, as seen in Figure 2.5. Copper-treated films showed fluorescence of 48.32 $\pm$ 1.45, and iron was nearly the same value at 47.35 $\pm$ 1.40. The results in Figure 2.5 confirm that there is metal ion binding activity at the surface of the copolymer, and that nickel is the most effective ion in binding hisGFP.

While the first experiment was designed to identify the most effective metal ion in binding the recombinant protein, the second test was designed to ensure that binding of the hisGFP was due only to the his_6 affinity tag on the protein N' terminus. Therefore, hisGFP and GFP without the his_6 affinity tag were tested against each other on identical films to show the importance of the his_6 tag to the copolymer surface binding in this system.

A baseline fluorescence value was established as in the previous test, and it was found that all experimental controls gave very similar fluorescence readings, which were averaged together and treated as the baseline, as seen in Figure 2.6. Data for the hisGFP and GFP on the non-metal loaded polymer was analyzed with ANOVA, which showed them to be statistically close to baseline, suggesting

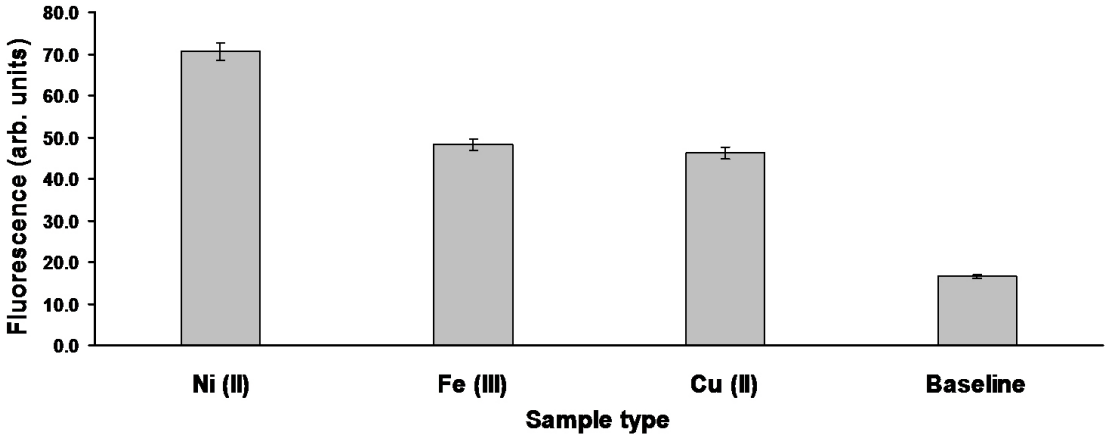

Figure 2.5: Fluorescence data obtained from block copolymer surfaces loaded with different metal ions and exposed to hisGFP. The Nickel-loaded block copolymer exhibited significantly higher affinity to his GFP than other metal-loaded polymer samples.

that the polymer with no metal had little or no affinity for either protein. ANOVA also showed that the nickel-loaded copolymer surface held a significant amount of the hisGFP with a detected fluorescence of 77.43 ± 8.74. The nickel-loaded polymer could not significantly bind the untagged GFP, as its fluorescent intensity was not significantly above baseline.

This data suggests strongly that the interaction between the hisGFP and the metal at the polymer surface is significantly higher than any other nonspecific interactions in the system, and that the metal-loaded surface is indeed specifically interacting with the his_6 affinity tag.

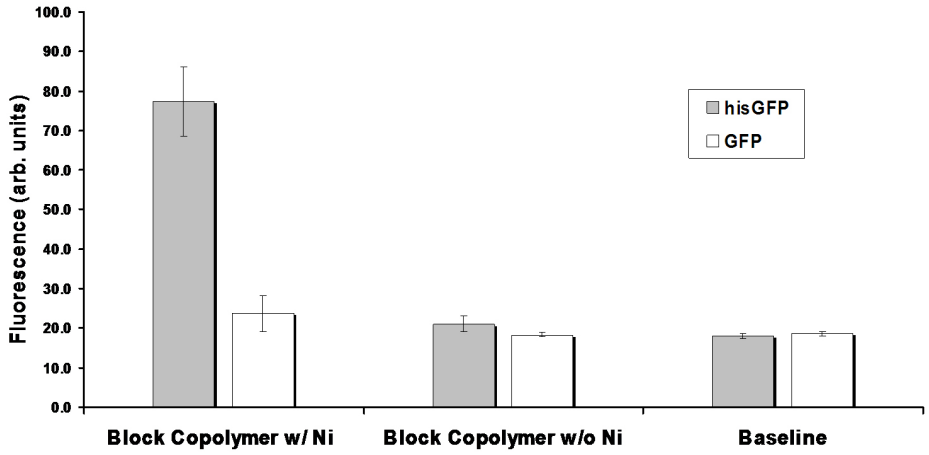

Figure 2.6: Comparison of hisGFP vs. GFP fluorescence on various surfaces. Only the fluorescence caused by hisGFP binding on the nickel-loaded block copolymer surface was significantly above baseline.

2.7 Conclusions

The experiments performed on this block copolymer system show that nickel is the most effective metal in chelating histidine-tagged green fluorescent protein, and that the metal-loaded surface of the norbornene block copolymer is capable of binding histidine-tagged green fluorescent protein while being unable to bind green fluorescent protein without histidine tags. While there are undoubtedly non-specfic interactions like hydrogen bonding and Coulombic attraction between the polymer, metal, and the target protein, it appears that only the histidine-metal chelated protein can remain through the process of washing performed in these experiments. Future work upon this project will focus on studying the

composition of the metal-loaded copolymer surface and the actual location of these histidine-tagged proteins on the copolymer surface.

2.8 Acknowledgment

This material is based upon work supported by the National Science Foundation and the Intelligence Community through the joint "Approaches to Combat Terrorism" Program DMR-0346253, and the United States Department of Agriculture National Research Initiative Competitive Grants Program (USDA-NRICGP) Grant # 2005-35603-15371.

Chapter 3

Nanopatterning of Tobacco Mosaic and Necrosis Virus Using Poly(styrene-*b*-4-vinylpyridine)

3.1 Introduction

This chapter will seek to show that similar principles used to nanopattern histidine-tagged green fluorescent protein (hisGFP) on the surface of the norbornene block copolymer can also be applied in a different block copolymer system with different biological species. The nanopatterning mechanism between the virus and copolymer differs from the histidine-nickel chelation that occurs between the histidine-tagged green fluorescent protein and the NOR/NORCOOH-nickel diblock copolymer. Analysis of this system showed that the histidine tagged added to the green fluorescent protein was responsible for its binding behavior. The virus species that were tested did not have a hexahistidine (his_6) tag, and required a different interpretation of the virus binding behavior.

Viruses are physically much larger than individual protein molecules, such as the tested his_6-tagged green fluorescent protein. For example, hisGFP is a single protein containing 238 amino acids, while the Tobacco mosaic virus is composed of 2130 surface protein subunits surrounding an RNA core of 6400 base pairs. Thus, the virus is about three to four orders of magnitude larger than the virus. The virus surface is composed of a multitude of protein subunits, each of which presents a particular set of functional groups. Non-tagged GFP was unable to bind to the surface of the NOR/NORCOOH block copolymer. This is because the histidine-nickel chelation binding is strong compared to the relatively weak non-specific functional group associations, such as hydrogen bonding and van der Waals attractions, occurring between the copolymer's surface molecules and metal ions and the external functional groups of the protein. With this result in mind, it is expected that these non-specific functional group interactions cannot account for significant binding of viruses to the block copolymer surface.

Rather, the binding between the virus and the copolymer occurs because of unlike-charge Coulombic interaction. The viruses proposed carry a net negative surface charge at neutral pH. The block copolymer, loaded with non-oxidized metal, should carry a net positive surface charge. It is assumed that this interaction will be the dominant mechanism of virus binding to the metal-loaded block copolymer surface. Previously, Tween detergent was used to test the specificity of GFP binding by disrupting weak, non-specific binding between the surface func-

tional groups on the protein surface at the nickel-loaded NOR/NORCOOH block copolymer. Here, Tween will also be used to examine the strength the binding of the virus to the copolymer surface by disrupting weak functional group interactions between the virus and the copolymer. Since it is theorized that the interaction between the virus and copolymer is Coulombic, viruses should remain on the surface after washing with Tween.

3.2 Background

Viruses are mobile genetic elements surrounded by a protein coat [72]. Since they cannot replicate themselves autonomously, they are obligate parasites that seek out host cells in order to reproduce. Viruses are able to induce the protein synthesis and assembly mechanisms of cells to in order to produce viral proteins that are assembled into functioning virions.

Viruses can infect many different kinds of cells, including bacteria, animal, and plant cells. They are able to do this by penetrating the cell membrane, or in the case of plants, through damaged cell walls. When the virus penetrates the cell, the viral genetic material in the form of DNA or RNA enters the cell and exploits the cell's own molecular machinery to replicate itself. The infected cell then reproduces and assembles the virus and its coat proteins according to the instructions written on the viral genetic code [72]. Generally, the production of viral proteins is harmful to the infected cell, and can be fatal.

The study and understanding of viruses and their interaction with other living organisms is crucial in improving standard of life, both from an epidemiological and economic perspective. Many human diseases, causing significant loss of life, are viral in origin. Viral respiratory infections and human immunodeficiency virus (HIV) are two examples of diseases with viral origin that claim millions of lives a year [73, 74]. Plant viruses are also a cause for serious economic concern. An example is the bean pod mottle virus, which destroys soybeans [72], and maize dwarf mosaic virus, which is a worldwide problem affecting corn crops. These viruses can cause problems with the food supply and affect economies around the world [75, 76], causing billions of dollars in lost or damaged crops.

Nanopatterned surfaces can be used to target viral surface proteins in order to study their structure and function more easily and more accurately. A nanopatterned surface has already been shown to affect the mobility and morphology of cells [85]. It is the purpose of this study to lay the foundations for a block-copolymer based nanopatterning system for identification and analysis.

3.2.1 Poly(styrene-*b*-4-vinylpyridine)

The PS/P4VP purchased from Polymer Source had a molecular weight ratio of 20.0K/19.0K for the polystyrene and poly(4-vinylpyridine) blocks, respectively. The polystyrene block had a degree of polymerization of 192, and the poly(4-vinylpyridine) had a degree of polymerization of 180. The total block copolymer

had a polydispersity of 1.09. The structure of PS/P4VP is seen in Figure 3.1.

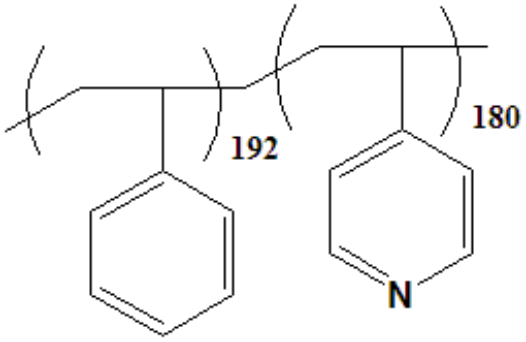

Figure 3.1: Structure of the poly(styrene-*b*-4-vinylpyridine) copolymer.

PS/P4VP was employed in these experiments because it has often been used in other published research to take up metal ions for various purposes [41, 42, 43]. Metal chelation occurs through the lone electron pair on the pendant pyridine moiety. At room temperature, both polystyrene (T_g 97.06 ℃) and poly(4-vinylpyridine) (T_g 143.65 ℃) blocks are in a glassy state limiting the diffusion of metal ions from poly(4-vinylpyridine) to polystyrene. Metal ion localization in the poly(4-vinylpyridine) is important to the nanopatterning process, because it insures that the tested viruses will be templated by the metal-loaded poly(4-vinylpyridine) block and not feel competing attraction to polystyrene due to unintended metal diffusion from block to block.

A lamellar block copolymer microstructure is expected when a film is cast from a non-specific solvent for both polystyrene and poly(4-vinylpyridine), which in this case was chloroform, as seen in Figure 3.2. Ni^{2+} does not dissolve in chlo-

roform, however. In order to dissolve both Ni^{2+} and PS/P4VP block copolymer, a solvent mixture of 8.5 % tetrahydrofuran and 91.5 % was used. The copolymer microstructure resulting from stating casting of this solvent mixture was cylindrical, as seen in Figure 3.3. Ni^{2+} binds to the P4VP block, causing the observed darkened cylinders in Figure 3.3. In this micrograph, both the cylinder ends and sides are visible. The long axis of the P4VP cylinders are approximately 20 nm in diameter, with an intercylindrical distance of approximately 20 nm and cylinder lengths greater than 1 μm. These dimensions should therefore be favorable for the nanopatterning of a similarly cylindrical virus, such as tobacco mosaic virus, which has a diameter of 18 nm and a length of 300 nm.

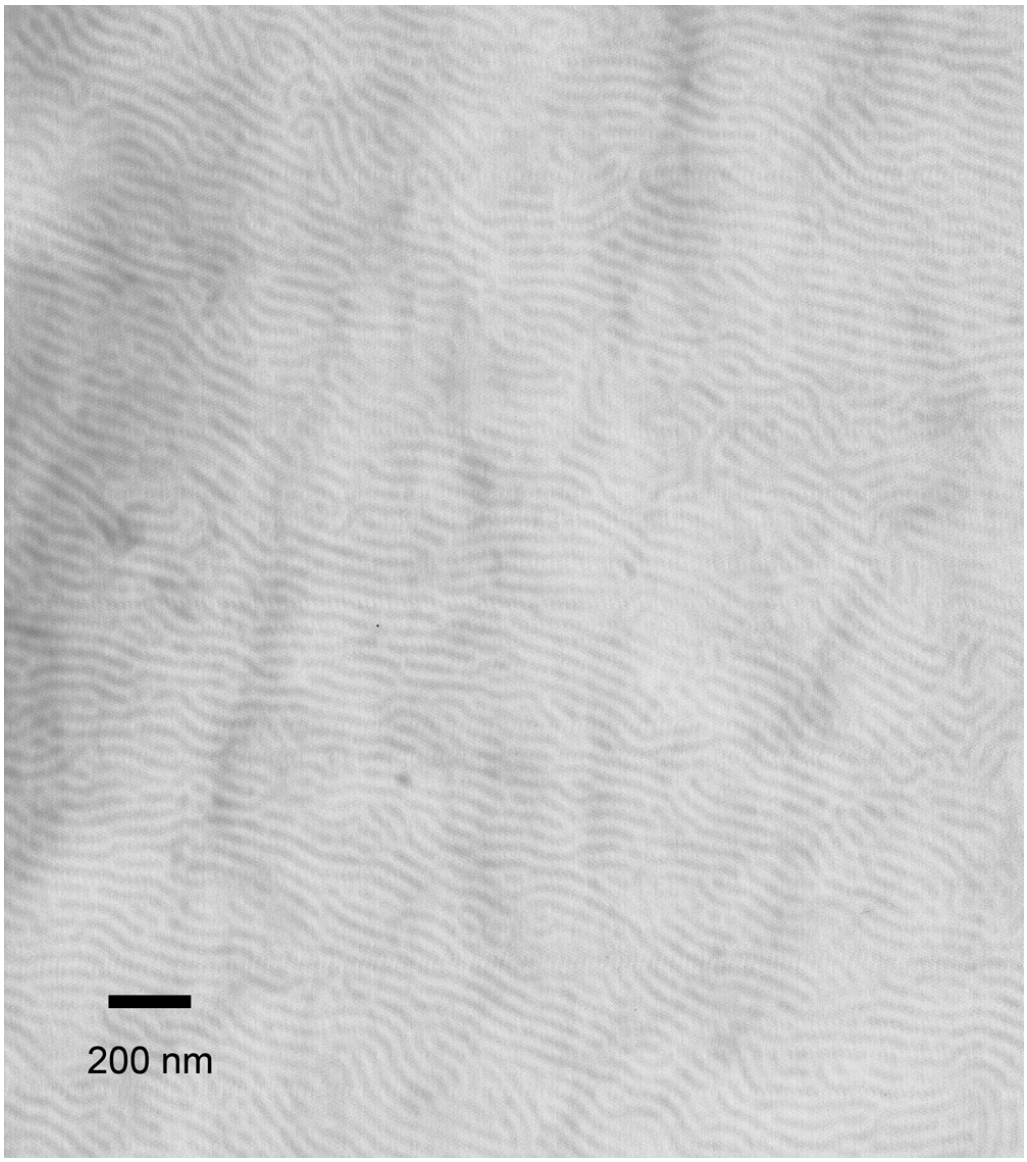

Figure 3.2: TEM micrograph showing lamellar microstructure of PS/P4VP when static cast from chloroform. Contrast between polystyrene and poly(4-vinylpyridine) is provided from iodine vapor staining.

Figure 3.3: TEM micrograph showing both the sides and the ends of the cylindrical microstructure resulting from PS/P4VP-Ni film formation from static casting from 8.5 % tetrahydrofuran and 91.5 % chloroform. The Ni^{2+} ion in the P4VP block provides contrast.

3.2.2 Tested tobacco virus species

Two different virus species were used in order to examine the interaction between viruses and the block copolymer surface. Tobacco mosaic virus (TMV) and tobacco necrosis virus (TNV) were used primarily for three reasons: they are very well characterized, they cannot infect humans, and they are easily synthesized in large amounts [83]. Tobacco mosaic virus is a common plant virus that infects tobacco leaves as well as a nearly 150 other herbaceous and dicotyledonous plants including tomato, pepper, spinach, and many flowers [80, 81]. Generally, infection causes stunting of the plant and reduces the amount of useful crop. The TMV virus is non-enveloped virus with a helical RNA strand of 6400 bases surrounded by a coat of 2130 identical coat proteins. The TMV virion is a rigid rod 300 nm long with a diameter of 18 nm (Figure 3.4). The isoelectric point of TMV is 3.5, so at pH 7, TMV has an overall negative surface charge, with a linear charge density of 0.5-2 electrons/Å [79]. TMV forms head-to-tail oligomeric strings that are much longer than the length of a single TMV virion (Figure 3.5).

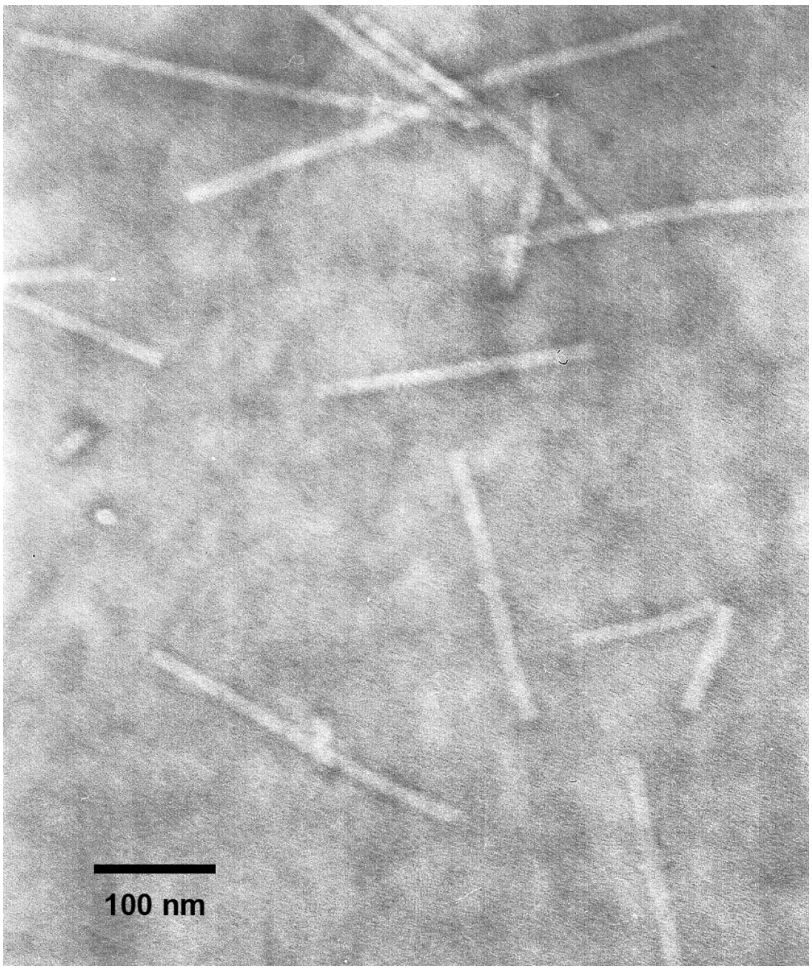

Figure 3.4: Electron microscope picture of the tobacco mosaic virus.

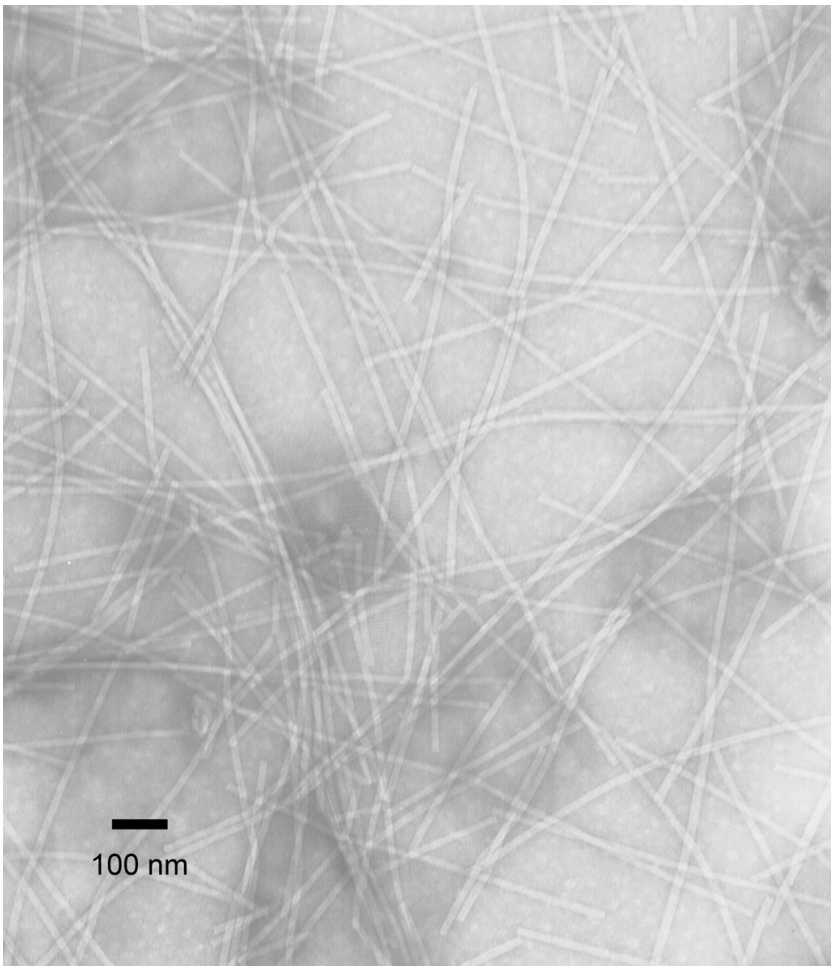

Figure 3.5: Oligomeric strands of TMV caused by head-to-tail addition.

Tobacco necrosis virus (TNV) is another plant virus affecting a large variety of commercial crops. Unlike the TMV rod, TNV has a regular icosahedral shape with an average diameter of 26 nm [77], seen in Figure 3.6. It is also a non-enveloped RNA virus, like TMV, and it will be used to further study the interaction of copolymer surface with virus. TNV has an isoelectric point of 4.5, so like TMV, TNV has a negative charge at pH 7. TNV is used to circumvent

the problem of multiple cylinder-virus interaction points. The long axis of the TMV virus does not always align with the long axis of a single cylinder, and often crosses many cylinders at an angle to the copolymer's preferred direction. Therefore, TNV gave the ability to study the behavior of single virions as they interacted with single copolymer cylinders.

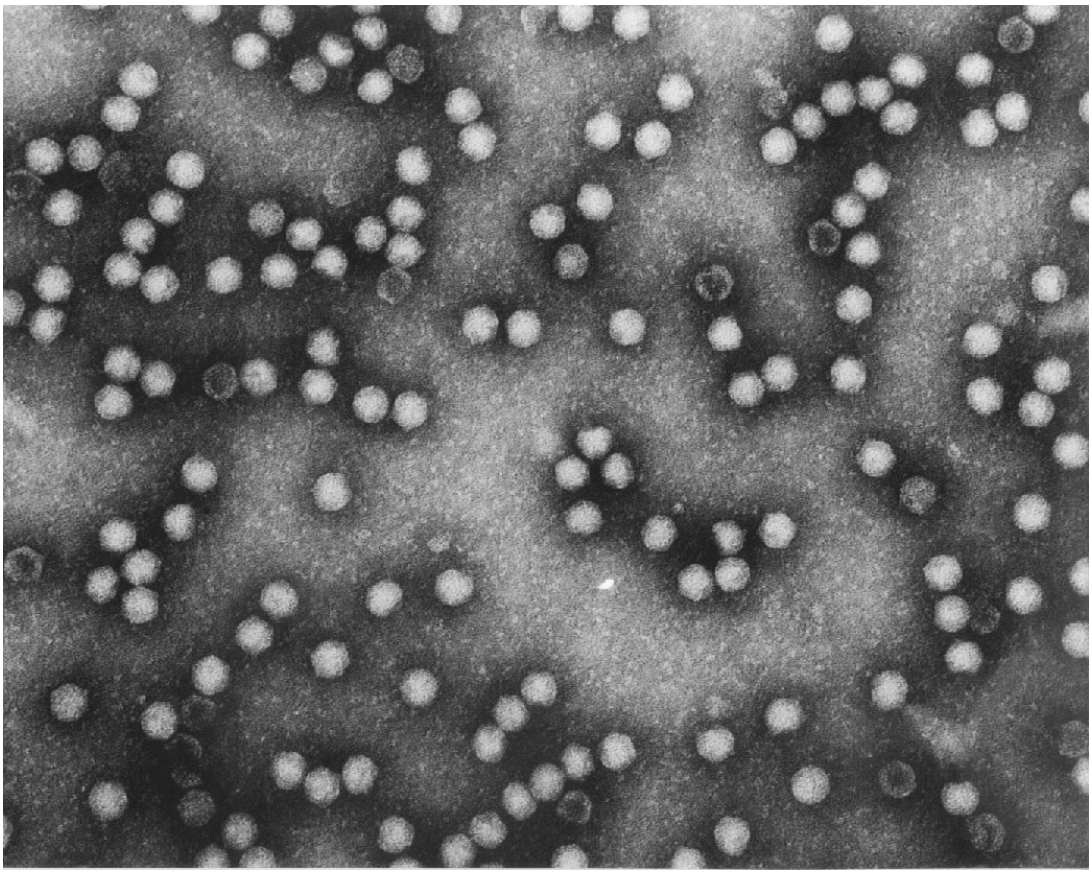

Figure 3.6: Tunneling electron microscope picture of the tobacco necrosis virus. Magnification is 300K [78].

3.3 Experimental design

3.3.1 Introduction

The purpose of experiments presented here was to deduce the mechanism of virus binding to the surface of the copolymer. With a better understanding of the nature of the virus-copolymer interaction, it was possible to then examine the patterning of the viruses on the surface of the block copolymer. Specifically, it was necessary to resolve the tendency of rodlike virus particles to lie randomly on the copolymer surface rather than self-orienting to maximize contact with the attracting block of the copolymer surface. To have any chance of large-scale ordering of the virus, the surface of the block copolymer itself must have a degree of long-range microstructural order. This was accomplished through the use of applied stress above the glass transition temperature. Tween detergent was again used to disrupt weak bonding between the copolymer and the virus. It is proposed that the interaction between the block copolymer and the virus is a Coulombic one, therefore Tween detergent will be used to eliminate the possibility of non-specific binding.

3.3.2 Ultramicrotoming and electron microscopy

A Leica EM UC6 Ultramicrotome was used to section samples for electron microscopy. PS/P4VP-Ni and PS/P4VP specimens were fixed in Spurr's fast-curing

resin. Embedded specimens were microtomed at room temperature. Specimens were cut to 100 nm thickness so that they would be visible in the TEM and be able to endure the planned virus exposure and Tween wash procedures. Microtomed films were mounted on 600 mesh copper grids, model number 600TT, purchased from Ted Pella. Electron microscopy was performed on a Hitachi H600AB electron microscope with 100 kV accelerating voltage.

It was found that samples thinner than 100 nm had two significant problems. They were damaged by the repeated water and detergent exposure, and they tended not to withstand the electron beam in the TEM and would curl away from the beam and break away from the grid. Therefore, all samples were cut to 100 nm for analysis.

3.3.3 Nickel metal complexation and film preparation of poly(styrene-*b*-4-vinylpyridine)

PS/P4VP was dissolved in chloroform, a good solvent for both polystyrene and poly(4-vinylpyridine). A polymer/chloroform concentration of 1 mg/mL was used. Nickel nitrate $Ni(NO_3)_2$ was dissolved in separate copolymer and solutions at a concentration of 100 μg/mL. In order to dissolve $Ni(NO_3)_2$ in the PS/P4VP/chloroform system, the metal salt was added to the solution and the mixture was titrated with tetrahydrofuran until a clear solution was formed. At the point of solution formation, the amount of tetrahydrofuran added was 8.5 %

of the total solution volume.

Bulk films of the copolymer and metal were cast in flat-bottomed basins formed from Bytac film in a chloroform-saturated desiccator in order to slow the evaporation process. Film formation through evaporation occurred slowly over the course of a week. These static cast films were further processed using stress applied in a heated channel die in order to give a preferential direction to the long axis of the PS/P4VP cylindrical microstructure. Binding analysis of the virus-copolymer system consisted of visualization through electron microscopy. Binding experiments were performed with the PS/P4VP films cut and mounted on 600-mesh copper TEM grids.

3.3.4 Stress-Induced Orientation of PS/P4VP-Ni Block Copolymer Morphology

A custom-made aluminum mold with integrated cooling water galleries was used to heat the copolymer past its glass transition temperature, transmit applied stress, and quench the copolymer once it experienced flow. A schematic of this die is shown in Figure 3.7. PS/P4VP-Ni films loaded into the channel die from static casting were translucent with a light blue color.

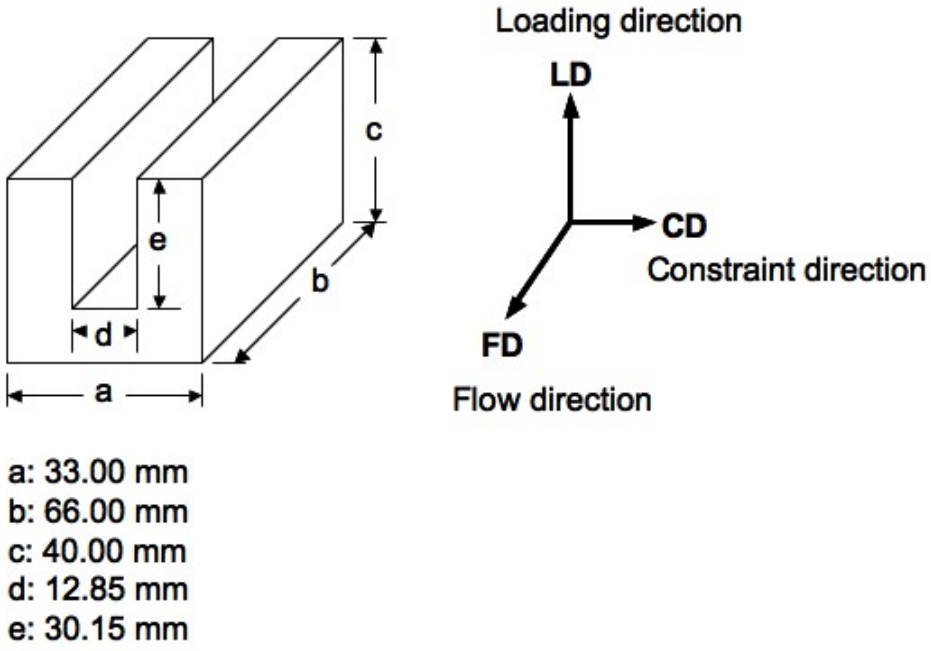

Figure 3.7: Dimensions of the channel die used to orient the PS/P4VP block copolymer. Also shown are the three major axes of deformation.

Samples were heated to 160 ℃ in a standard Carver 2400 digitally controlled heat press. A small pre-loaded force of about 100 lbs was initially applied to

the cold sample prior to flow to ensure proper mechanical and thermal contact of the channel die with the copolymer. Flow initiated when the preload pressure was observed to drop to zero, indicating the copolymer could no longer support a mechanical load. This occurred shortly after reaching the target temperature of 160 ℃ . Pressure was immediately raised to 2000 lbs and the copolymer was allowed to flow until it reached the ends of the mold. At this point, the heaters were turned off and cooling water was flowed through the mold, dropping the system temperature to room temperature at a rate of approximately 280 ℃/min. The applied pressure was maintained during the quenching process. Once cool, the copolymers were removed from the mold after being carefully marked to show the direction of flow.

3.3.5 Virus Staining Technique

Electron microscopy was the analytical tool used to examine the morphology of the block copolymer and virus species. In order to properly image the virus, a stain was applied to provide contrast in the electron beam. Commonly, phosphotungstic acid (PTA) is used when staining TMV and TNV. It was found, however, that PTA caused significant interference with the existing block copolymer contrast, as in Figure 3.8 . The tendency was for the virus to be weakly stained, accompanied by a loss in contrast from the metal-containing microstructure of the copolymer.

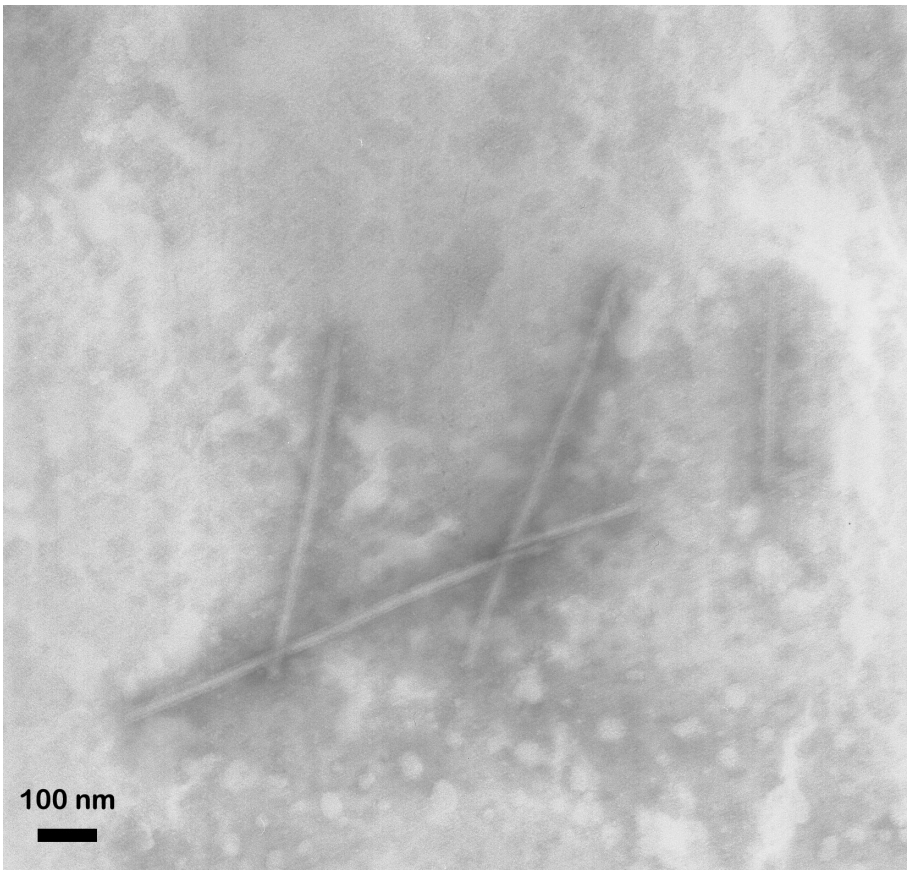

Figure 3.8: Image of TMV stained with phosphotungstic acid. The underlying PS/P4VP copolymer with nickel-containing microstructure is obscured by over-staining with phosphotungstic acid.

A successful alternative was to stain the block copolymer/virus system with a 1 % solution of uranyl acetate (UA) [82]. When applied to the block copolymer/virus surface, UA was able to clearly show virus particles while not interfering with the visualization of the block copolymer microstructure. The staining procedure was always a 30-second exposure to a 1 mg/mL solution of UA.

Staining was performed by holding the grid of interest containing the copoly-

mer film in self-closing tweezers and allowing a 10 μL drop of UA staining solution to rest on the surface for 30 seconds. At the end of the stain time, the drop was rapidly removed by gently contacting the grid bottom and sides with filter paper. Once the stained film was fully dry, it was allowed to air-dry for at least 30 minutes before insertion into the TEM.

3.3.6 Binding of Tobacco Mosaic Virus on PS/P4VP-Ni and PS/P4VP

The TMV binding ability of the PS/P4VP-Ni surface was tested by directly exposing TEM-grid mounted samples to an aqueous TMV solution. In order to test the binding strength of TMV to the metal-loaded copolymer surface, detergent washes were performed in order to analyze the amount of virus held by the copolymer. Initial TEM pictures were taken to establish the appearance of the TMV on the copolymer surface. Tween detergent was used to attempt to clean the copolymer of TMV.

Wild type TMV was prepared according to literature procedures [83]. Samples of PS/P4VP-Ni and non-nickel PS/P4VP were mounted on copper TEM grids as per the stated sample preparation method. A 10 μL droplet of the TMV solution of approximately 0.1 % mg/mL was placed on the grid and allowed to remain there for 1 minute. After 1 minute, the droplet was wicked away with filter paper. The sample was then immediately exposed to a 10 μL droplet of

uranyl acetate stain for 30 seconds, and then wicked away with filter paper. Once dry, the specimen was ready for electron microscopy.

Tween detergent washes were performed after virus exposure and before uranyl acetate staining. Primary washes consisted of a Tween-only solution. For Tween washes of 2 minutes or less, the TEM grid containing microtomed copolymer was held in tweezers and gently circulated in a basin of 1 % Tween for the required time. After exposure, the grid was wicked dry, rinsed with 10 μL of water, and wicked dry again. Upon drying, the washed sample was stained by exposing the grid to 10 μL of UA for 30 seconds.

For Tween washes lasting longer than 2 minutes, the grids were washed in autoclaved 1.5 mL centrifuge tubes. The tube was filled with 1 mL of the Tween wash solution. The grid containing copolymer and virus was dropped into the centrifuge tube, being sure that it did not float on the surface, but rather sank to the bottom. This centrifuge tube was then gently tumbled for the desired wash time. The sample was then rinsed with 10 μL of water, wicked dry, and then stained for 30 seconds with 10 μL of UA. Tween washes were also performed with a mixed solution of 1 % Tween and 1 molar sodium chloride (NaCl). Washing procedures for the Tween/NaCl solution were identical to those used for Tween-only washes.

3.3.7 Flow-induced exposure of tobacco mosaic virus to PS/P4VP-Ni

PS/P4VP-Ni films were prepared according to previous film preparation/microstructure stress alignment methods. Films were applied parallel to each other on the surface of the copper TEM grid. An apparatus was built that held the edges of the TEM grid and allowed the surface of the grid to remain unclamped, lying at a 45° angle to the horizontal countertop. A 1 mL sterile syringe was loaded with 1 mg/mL TMV solution. A flat-tipped Luer-locking needle was attached to the syringe. This syringe and tip were inserted into a syringe pump set to 3 mL/min pump rate. A schematic of this setup is seen in Figure 3.9. The TMV was flowed onto the surface of the TEM grid at 3 mL/min. When the TMV solution was spent, the grid was wicked dry, gripped in tweezers, and then exposed to UA for 30 seconds, as in previous experiments. TEM analysis of the flow experiment followed after a 30 minute drying period.

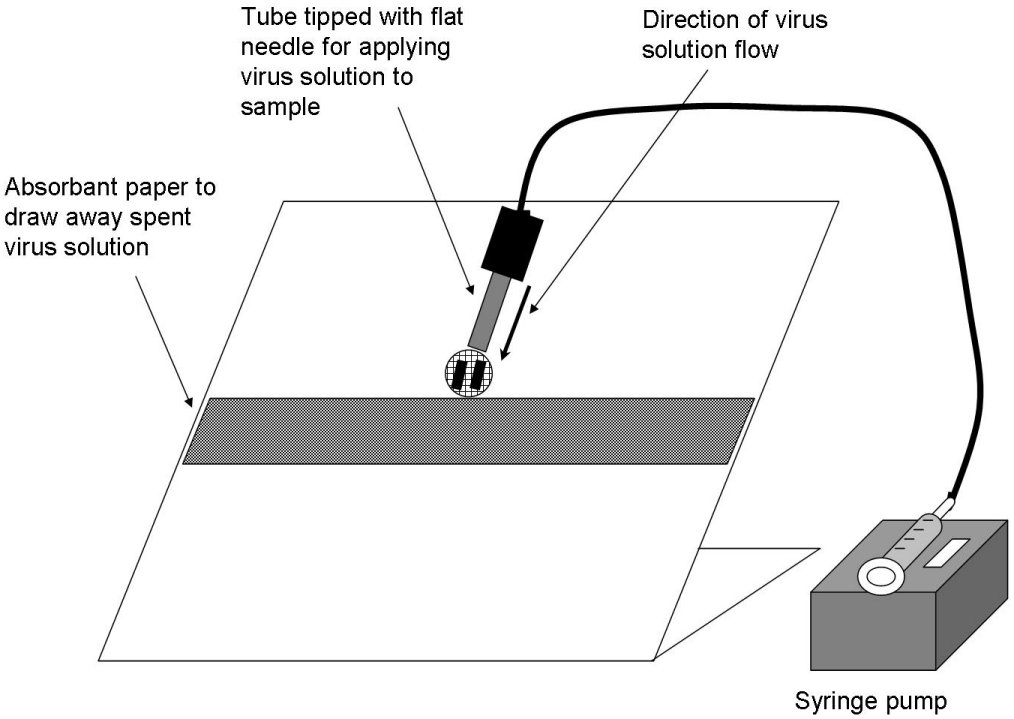

Figure 3.9: Schematic of the dynamic exposure apparatus built for exposing PS/P4VP-Ni films to flowing TMV solution. A syringe pump is connected to a tube which ends in a flat-tipped needle. At the barrel of the needle, a TEM grid with affixed microtomed sections of PS/P4VP-Ni is held stationary. The TEM grid is oriented so that the long axis of the copolymer points in the direction of virus solution flow.

3.3.8 Binding of tobacco necrosis virus on PS/P4VP-Ni

TMV, because of its 300 nm length, often lays across several cylinders, and therefore it is unable to help determine the effect of a single cylinder on the

binding activity of the surface. To this end, wild-type TNV was prepared through standard methods of tobacco leaf infection and purification [83] and was dissolved in a solution of approximately 1 mg/mL. Microtomed samples of oriented nickel-PS/P4VP were mounted on copper TEM grids and held in tweezers. As before, a 10 μL drop was allowed to remain on the surface for exactly 1 minute and then wicked away with a filter paper.

UA was used to stain TNV in an identical procedure to TMV. The sample was exposed to a 10 μL droplet of uranyl acetate stain for 30 seconds following TNV exposure, and then wicked away with filter paper. Once dry, the specimen was ready for electron microscopy.

3.4 Results and discussion

Preferential orientation of the copolymer microstructure was achieved by exerting pressure on the block copolymer above its glass transition temperature. Heat and flow of the block copolymer within the channel die had the effect of giving a preferential direction to the long axis of the cylinders formed through microphase separation of the PS/P4VP-Ni copolymer.

The partial orientation of the block copolymer microstructure was visualized through electron microscopy. Samples microtomed parallel to the flow axis, seen in Figure 3.10, showed only the sides of the cylinders, preferentially aligned in the flow direction. Samples microtomed parallel to the constraint direction, as

in Figure 3.11 showed only the hexagonally close-packed ends of the cylinders. For virus testing, it was desired to use the cylinder long axis. Therefore, following samples were microtomed to expose the cylindrical long axis of the block copolymer, and these surfaces were used in virus binding tests.

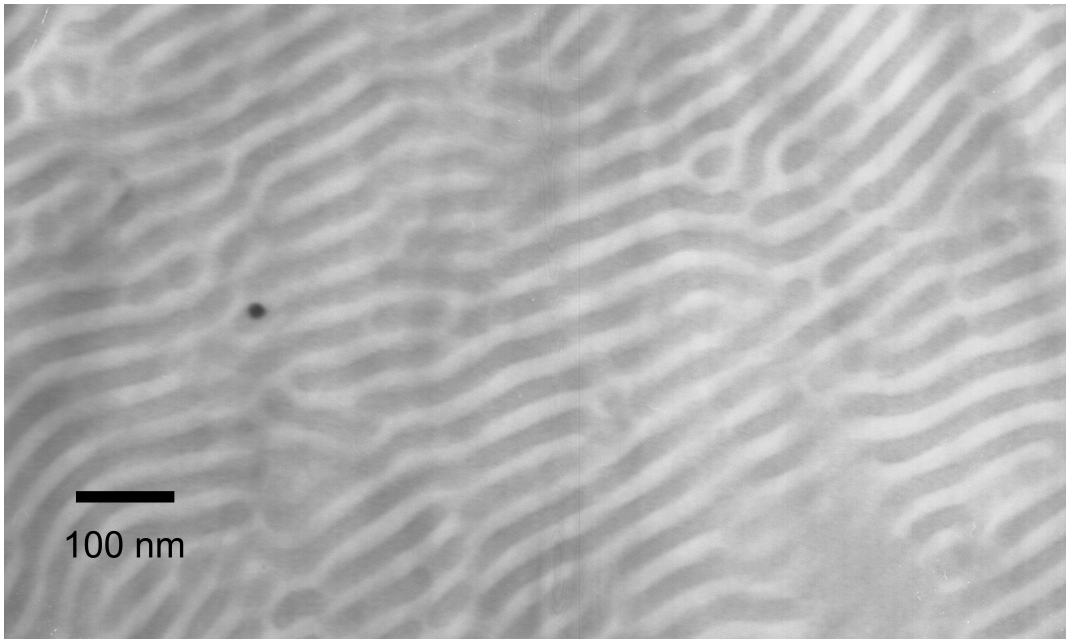

Figure 3.10: PS/P4VP-Ni microtomed along the flow direction, showing preferentially oriented cylinders. Contrast comes from nickel in the P4VP block.

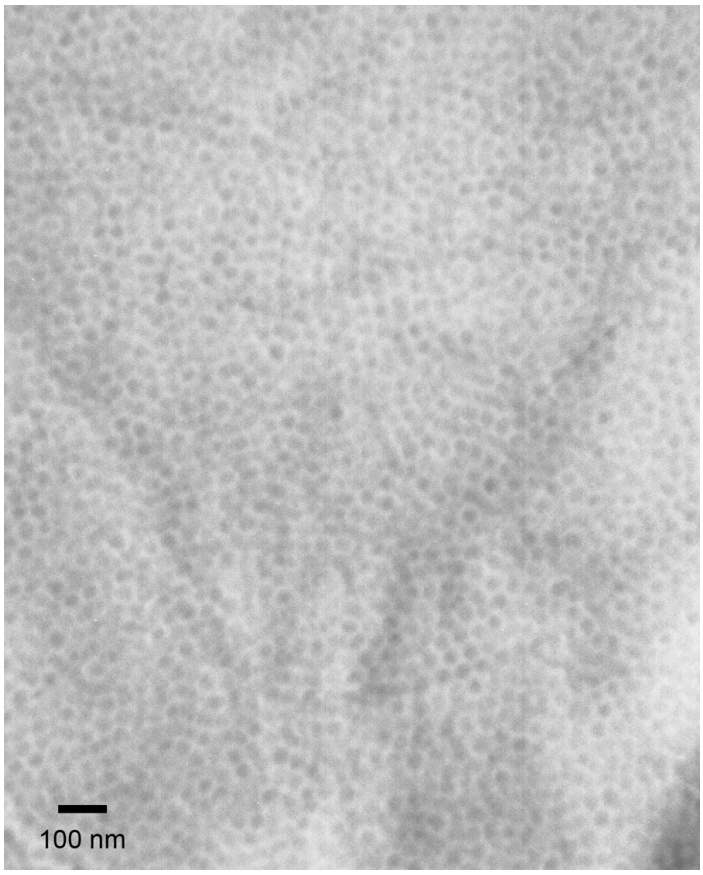

Figure 3.11: PS/P4VP microtomed along the constraint direction, showing the cylinder ends. Contrast comes from nickel in the P4VP block.

TMV was bound by the nickel-loaded PS/P4VP-Ni block copolymer preferentially over the non-metal-loaded PS/P4VP. As observed in the TEM micrograph in Figure 3.12, TMV remained visible on the block copolymer microstructure against 1 % Tween washes of up to 5 minutes, as seen in Figure 3.12. It was also seen that after extended washes of up to 2 hours, some scattered TMV was still observed on the block copolymer. Only after a 30 minute exposure to Tween, in Figure 3.14 was the visible TMV removed from the PS/P4VP-Ni surface.

PS/P4VP that was prepared without nickel was seen to lose almost all visible TMV before 2 minutes, as in Figure 3.13. In order to view the microstructure of the block copolymer, the polymer was stained after microtoming with a 2 hour exposure to iodine vapor, preferentially contrasting the P4VP block. TMV is observed on the non-metal PS/P4VP surface, in Figure 3.13. After one minute of Tween wash, approximately 55 % of the TMV is removced, and after 2 minutes in Tween, virtually no virus is seen on this surface as in Figure 3.13.

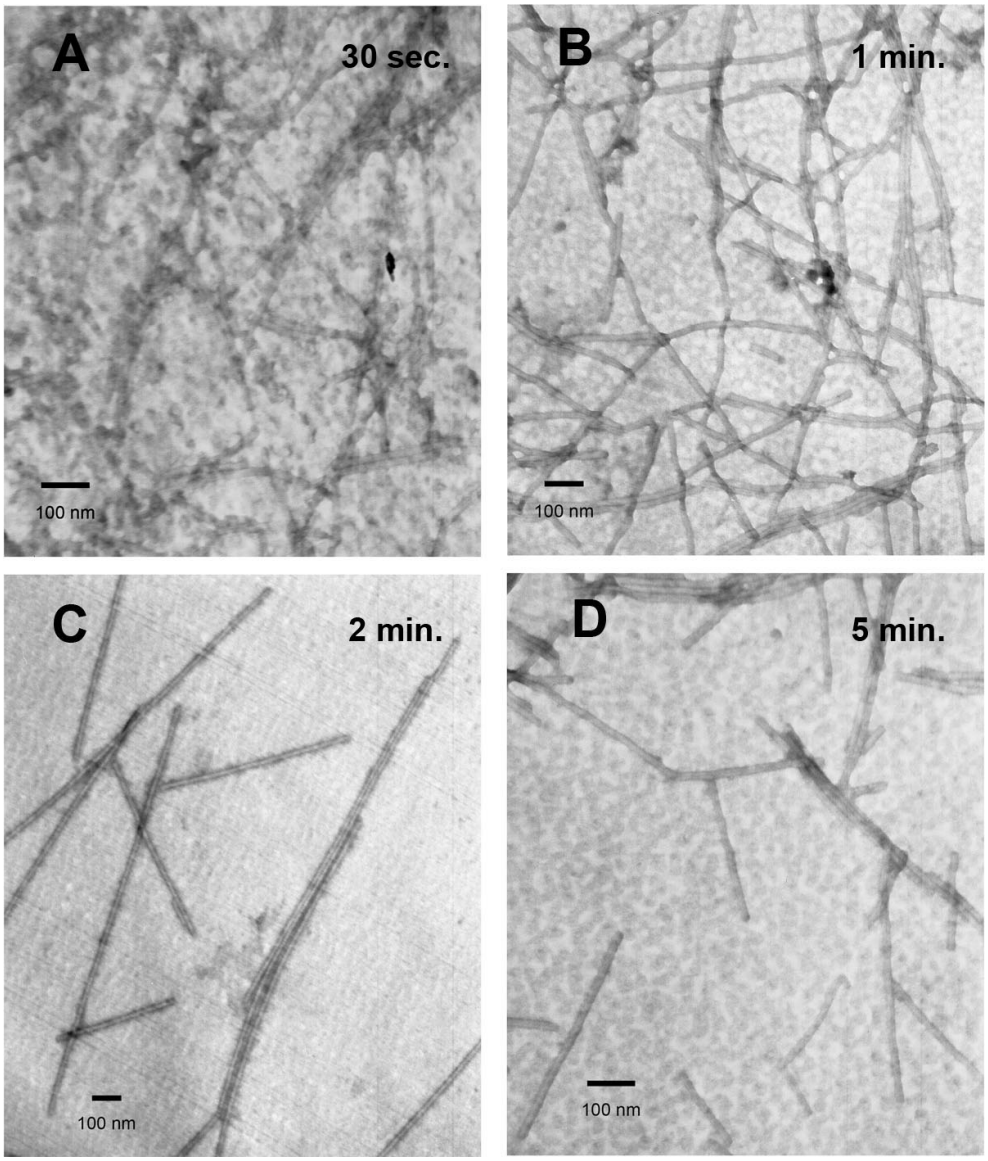

Figure 3.12: TEM micrograph showing TMV binding to PS/P4VP-Ni. The pictures are taken after increasingly long Tween washes. In 3.12A, wash time is 30 seconds, 3.12B is 1 minute, 3.12C is 2 minutes, and 3.12C is 5 minutes. After 6 hours, the surface still resembles that seen after 5 minutes, with some virus still visible.

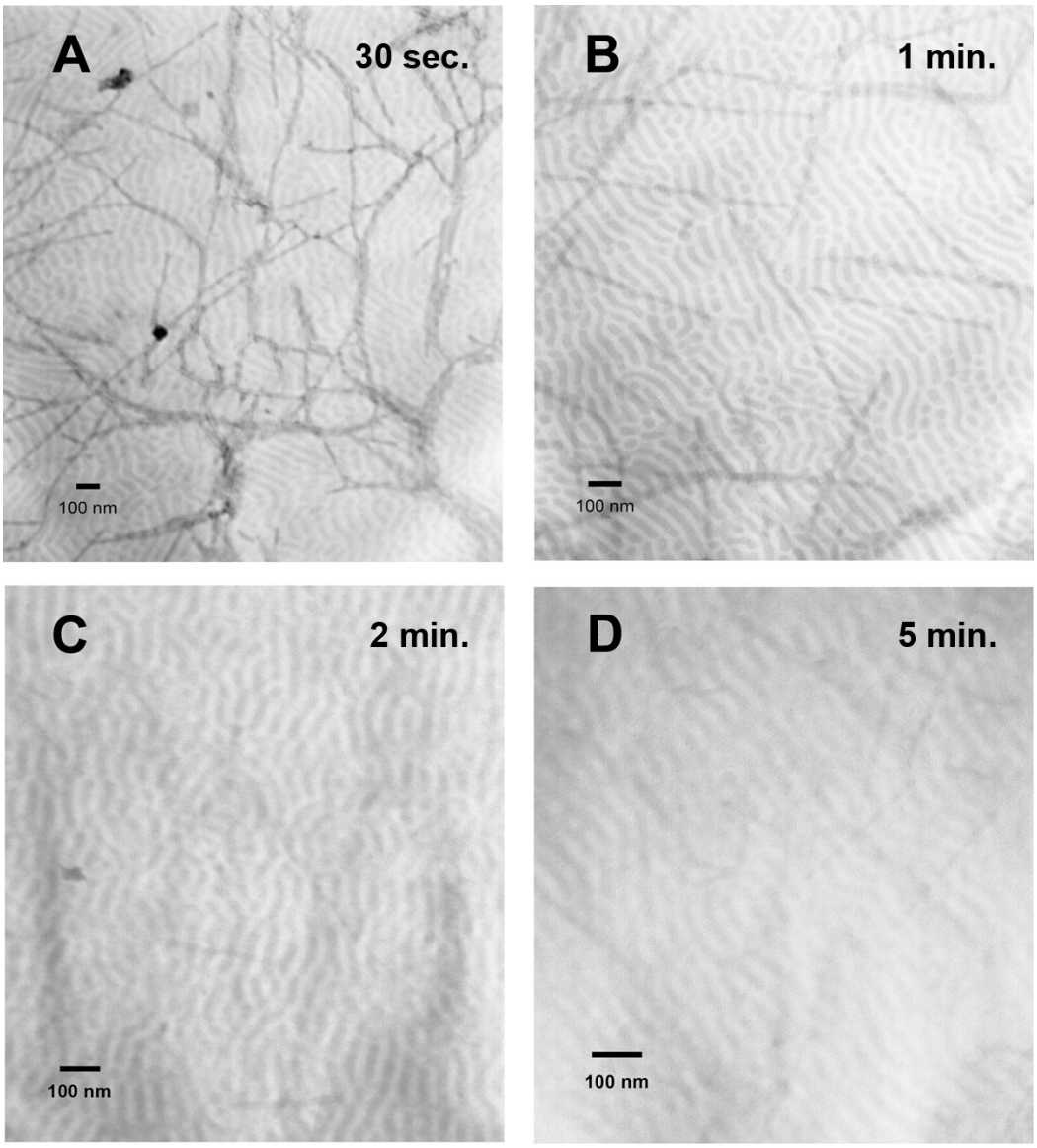

Figure 3.13: Binding of TMV to PS/P4VP with no metal loading. Contrast in this TEM micrograph comes from post-virus exposure staining of the P4VP block with iodine vapor. As in Figure 3.12, wash time in A is 30 seconds, B is 1 minute, and C is 5 minutes. In C, after a 5 minute exposure to Tween detergent, the virus is removed, leaving shadowy imprints but no visible virus particles.

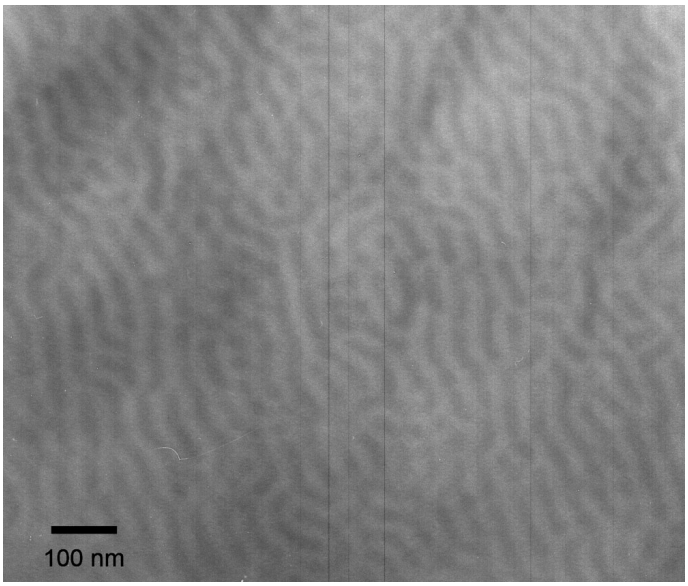

Figure 3.14: PS/P4VP-Ni surface following a 30 minute Tween detergent wash after TMV exposure. TMV rods are no longer visible on the surface, although there are shadowy remnants of the virus stained by UA. This indicates that the majority of TMV removal occurs before 30 minutes.

A sample of PS/P4VP-Ni, which had been exposed to TMV, was only partially dipped into the 30 % Tween solution and held there for 5 minutes. Tween 20 is typically used in concentrations ranging from 0.05 % to 0.5 %. As seen in Figure 3.15, there was near total virus removal from the washed portion, and there was a clear demarcation line between the washed and unwashed portion of the grid. While this unusually strong wash was able to remove viruses completely and noticeably from the copolymer surface, it is also possible that the Tween detergent, in very large concentrations, was able to shield the charge in-

teraction between the virus and the copolymer and facilitate its physical removal. Therefore, this result does not necessarily rule out the possibility of Coulombic unlike-charge based binding.

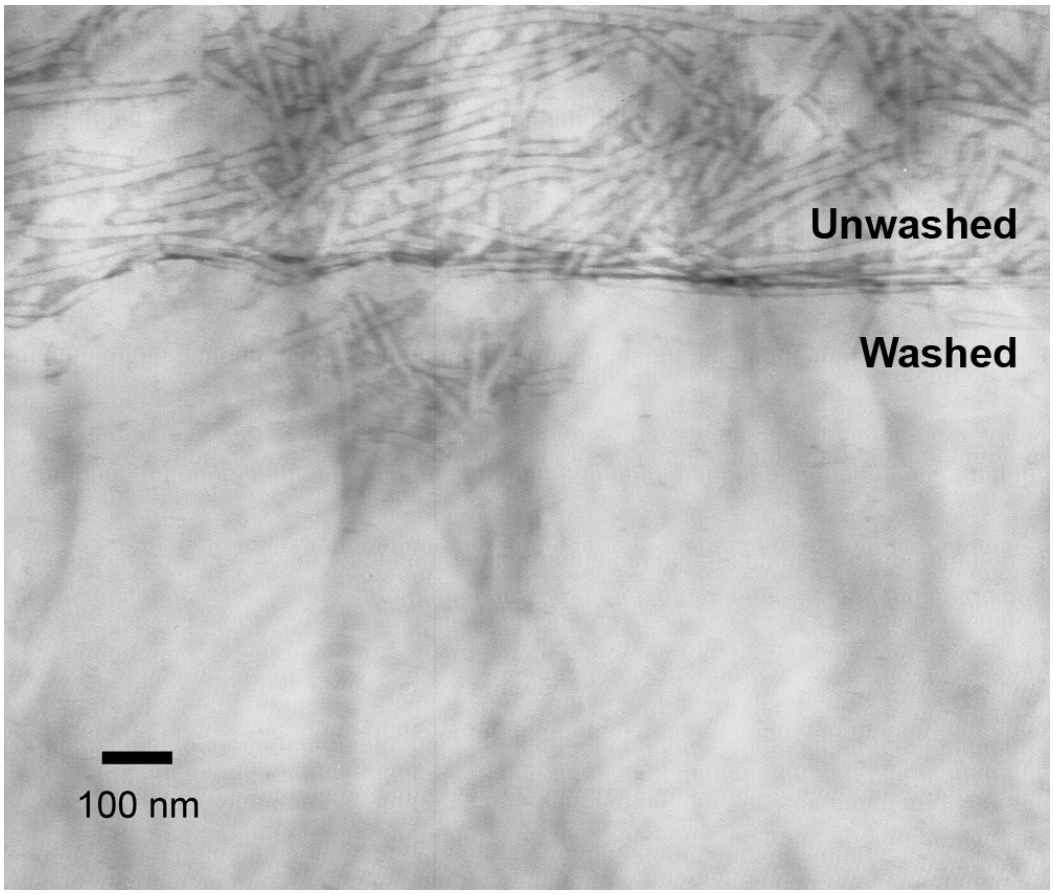

Figure 3.15: Border between washed and unwashed sections of a the TMV-exposed PS/P4VP-Ni surface after exposure to 30% Tween for 5 minutes.

The epoxy used to fix the PS/P4VP and PS/P4VP-Ni block copolymer was also examined for the presence of TMV. This compound is generally crosslinked and unreactive, and cannot participate in any significant binding with TMV.

Since it was also exposed to TMV, unwashed samples showed TMV present on the epoxy. However, once Tween washes were begun, the virus seen in Figure 3.13A and Figure 3.13B quickly diminished and was not seen on the epoxy after more than 2 minutes of 1 % Tween wash. The epoxy is a highly crosslinked network that is assumed to have little or no binding ability, similar to the polystyrene portion of the PS/P4VP block copolymer.

The disappearance of TMV from the epoxy shows that Tween is effective in removing non-specifically bound viruses. This result seems to indicate that although there should be significant non-specific binding, owing to the large number of the virus surface functional groups interacting with the surface, the dominant binding force holding the virus on the surface is either Coulombic binding of the negatively charged virus to the metal-loaded microstructure of the copolymer surface, or a result of chelation between the virus and nickel ions on the copolymer surface.

TNV was tested for its binding on nickel-PS/P4VP. While it is a much smaller virus than TMV, TNV is similar in that it carries a negative charge at pH 7. Because of its size, approximately 26 nm, it is possible for the TNV particles to fit within the confines of the metal-loaded P4VP portion of the surface microstructure. This makes TNV an excellent candidate for testing the binding of individual viruses to each separate block copolymer cylinder.

As in Figure 3.16, single TNV virions were seen to fit within both the PS

and P4VP portions of the copolymer surface microstructure. When exposed to wash, TNV associated with PS was washed away. Here, Tween 20 functions properly to solubize the TNV virions which have nothing specifically to bond to on the polystyrene portions of the copolymer surface morphology. There was a distinct correlation of the binding ability of single nickel-loaded P4VP cylinders, and individual TNV virions. This is important because it suggests that unlike charge binding occurs between the metal-loaded copolymer and the virus without the need for collective action between different P4VP-Ni cylinders. Again, as in the TMV tests, TNV was seen to bind to the nickel-containing PS/P4VP block copolymer surface following Tween 20 washes, adding further credibility to the Coulombic interaction explanation of TMV and TNV virus binding.

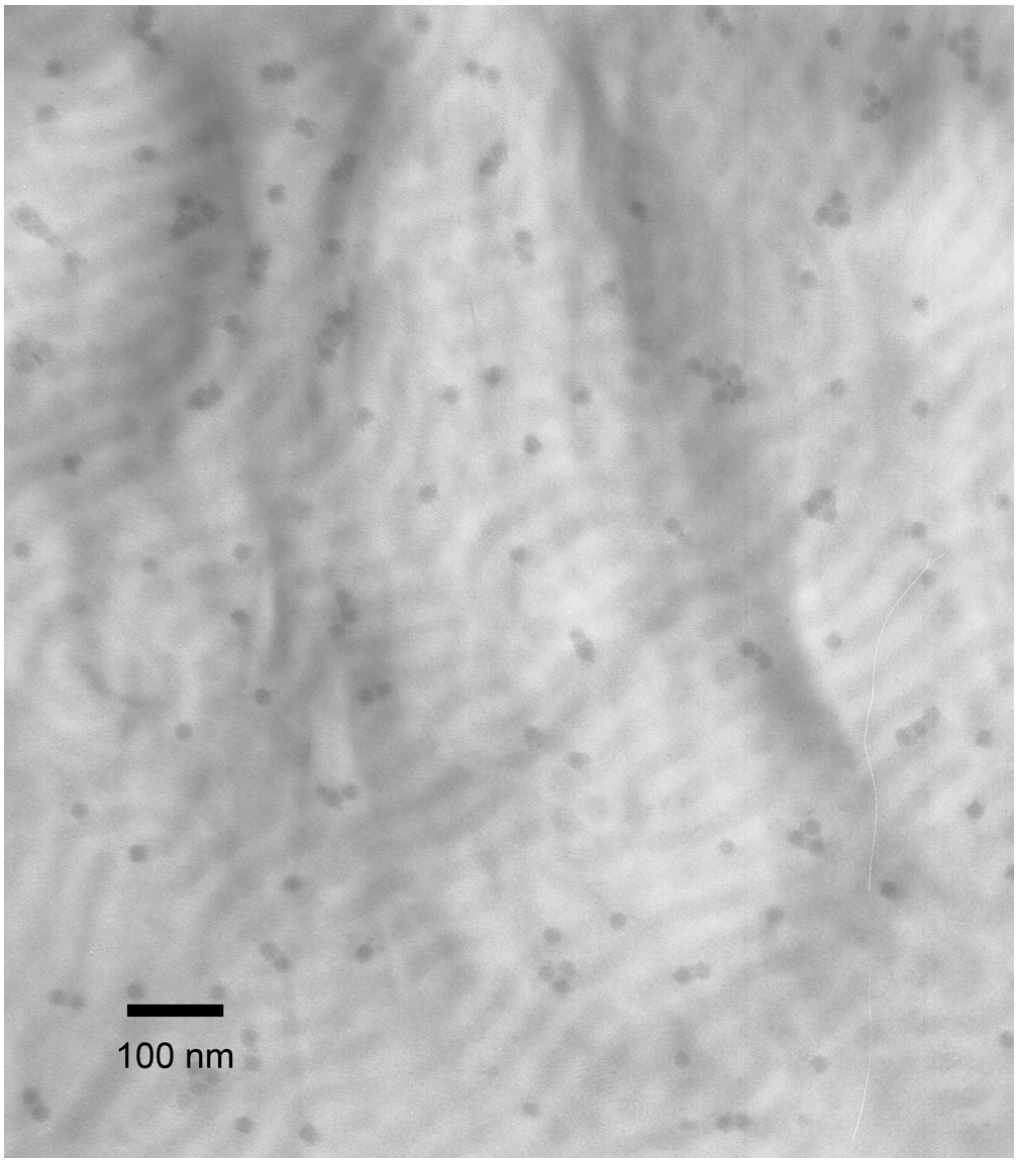

Figure 3.16: TNV on the surface of the nickel-loaded PS/P4VP-Ni block copolymer.

Tween washes were performed on TNV as they were on TMV, and it was seen that results were consistent with results achieved by washing TMV with Tween. When exposed to PS/P4VP-Ni, the TNV was not removed completely after 5

minutes in a Tween wash, although there is continuously less and less virus over time. Figure 3.17 shows TNV resisting Tween washes in a similar manner to TMV.

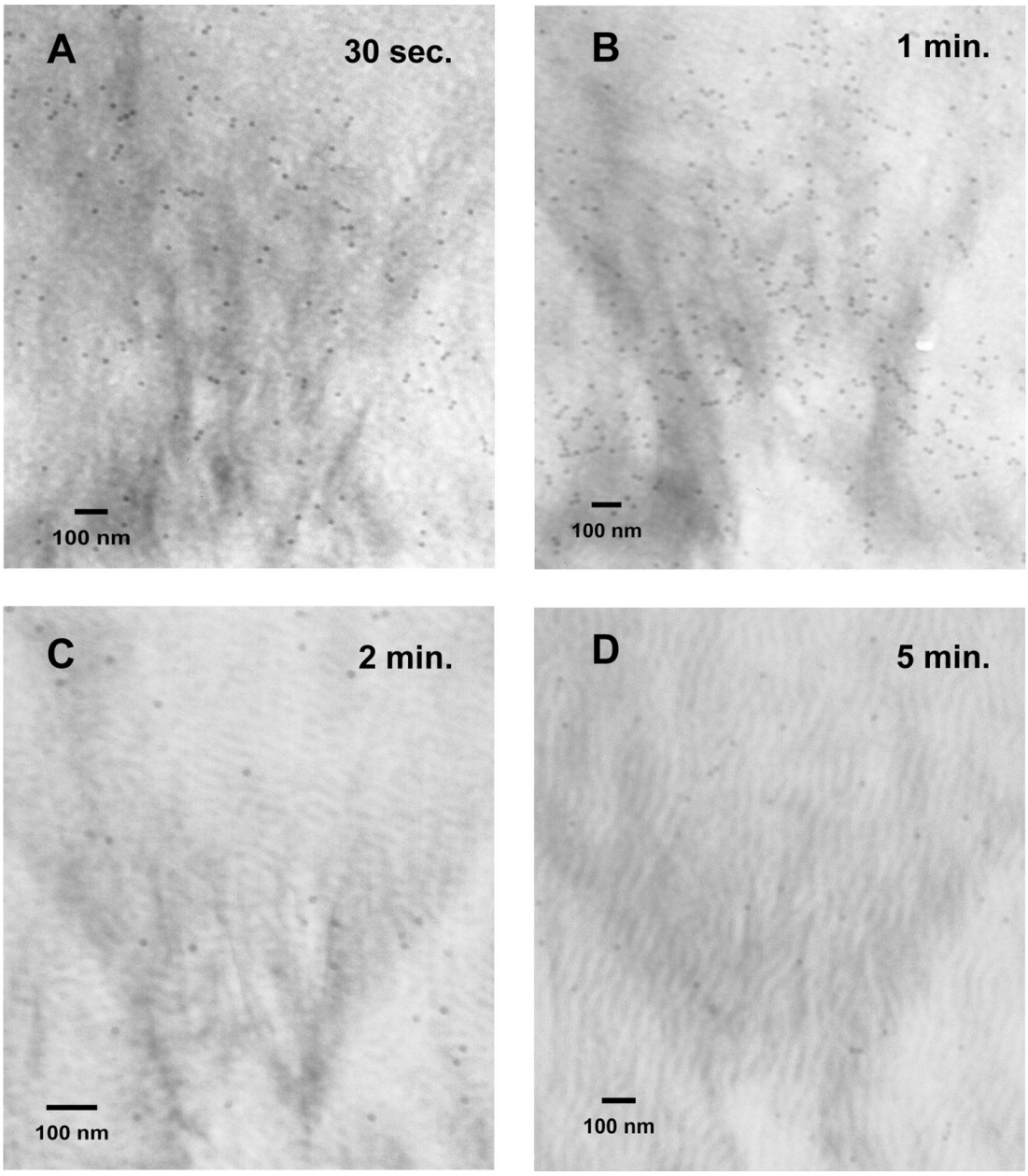

Figure 3.17: Effect of Tween washes on the presence of TNV on the surface of PS/P4VP-Ni. As in TMV binding, 5 minutes of wash is not sufficient to remove all visible TNV from the surface.

After one minute in the Tween wash, it was observed that TNV had been

mostly removed from the non-metal containing polystyrene portion of the block copolymer microstructure. TNV virions were clearly observed contained within the nickel-loaded 4-vinylpyridine cylinders. This is another positive indication that the virus does not bind through van der Waals or hydrogen bonding, but rather that the TNV specifically prefers the metal-loaded microstructure. The binding of TNV to the surface allowed observation of how individual viruses responded to individual parts of the block copolymer microstructure. Analysis of TNV micrographs showed that 87 % of the TNV particles, after a 2 minute Tween wash, were adhered to the nickel-conaining P4VP block of the copolymer. This large percentage of TNV-metal binding further suggests that the PS block is unable to bind TNV. With the possibility of virus binding to PS reduced, it seems likely that the virus particles are binding only to the nickel-containing P4VP block.

Non-nickel PS/P4VP was unable to show binding of TNV, as it did with TMV. Unoxidized nickel ions on the freshly microtomed PS/P4VP-Ni surface are assumed to carry the positive charge necessary for binding the TMV and TNV virions. PS/P4VP films, lacking the nickel ion and necessary positive charge, cannot strongly bind TMV or TNV.

Another interesting observation is the partial alignment of the TMV virion with the block copolymer microstructure, achieved with the help of shear caused by virus solution flow. When static cast, the TMV virions were seen to lie at all

angles randomly, with no preferred direction. The experiment involving dynamic exposure was performed with the flow direction coinciding with the long axis of the block copolymer. It was thought that this arrangement would make the TMV virions more likely to align with this long axis. As seen in the closeups in Figure 3.18 and Figure 3.19, this situation is indeed possible, as single virions were seen to match up well with the block copolymer's microstructure. Seen from a lower magnification, in Figure 3.20, a large-scale ordering of the viruses can be seen.

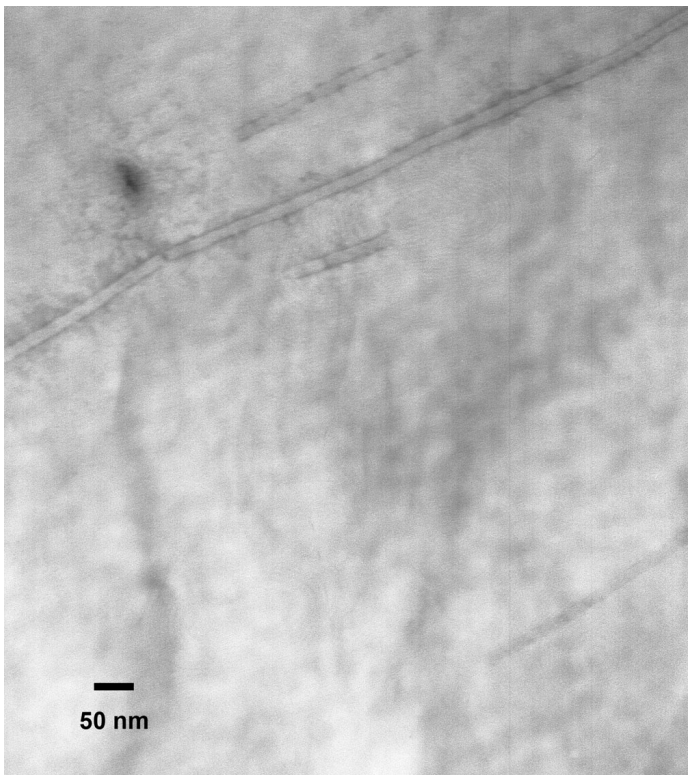

Figure 3.18: TEM micrographs showing alignment of single virions directly parallel to the flow axis of the PS/P4VP-Ni block copolymer microstructure.

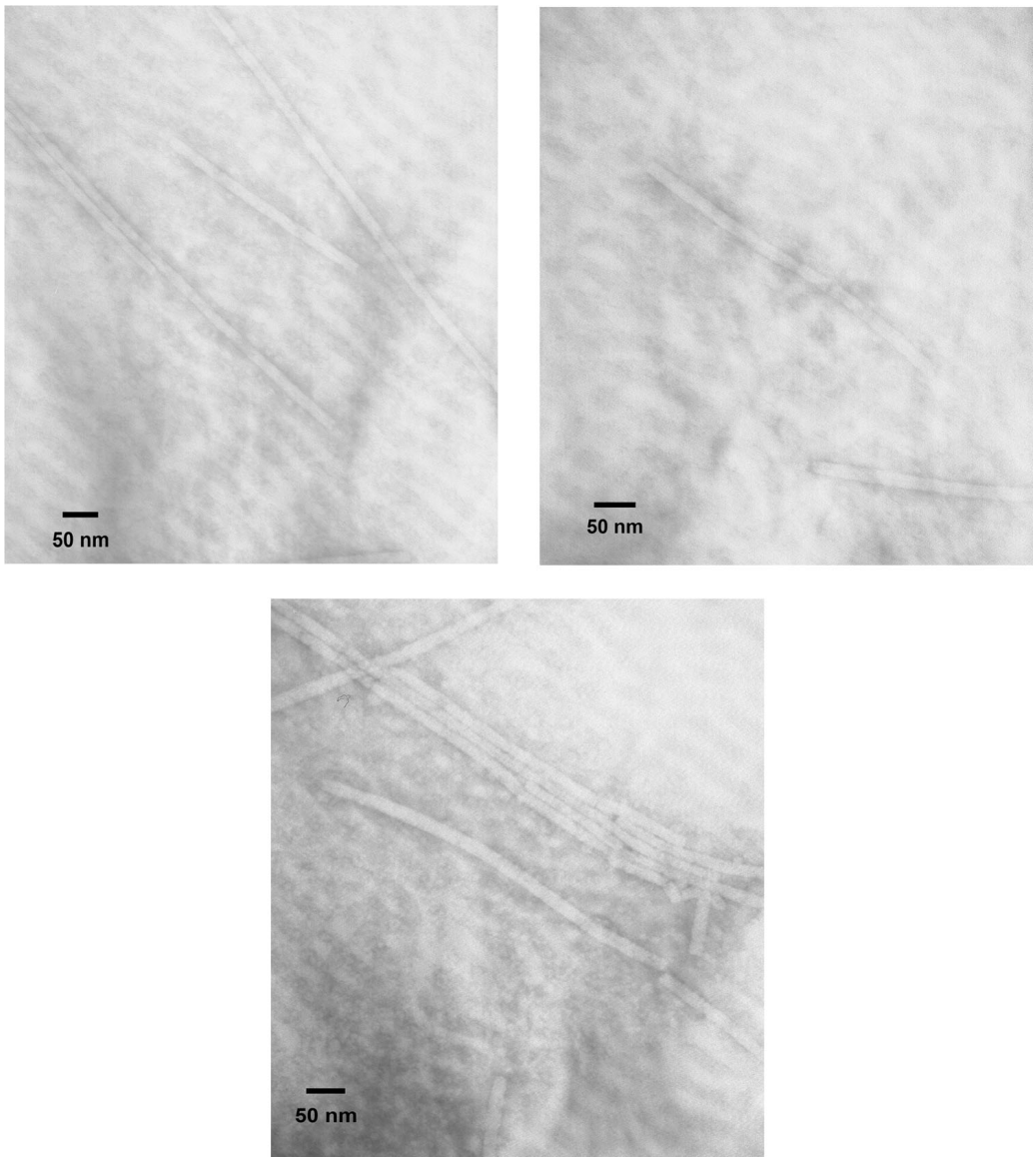

Figure 3.19: Other views of the TMV alignment with PS/P4VP-Ni.

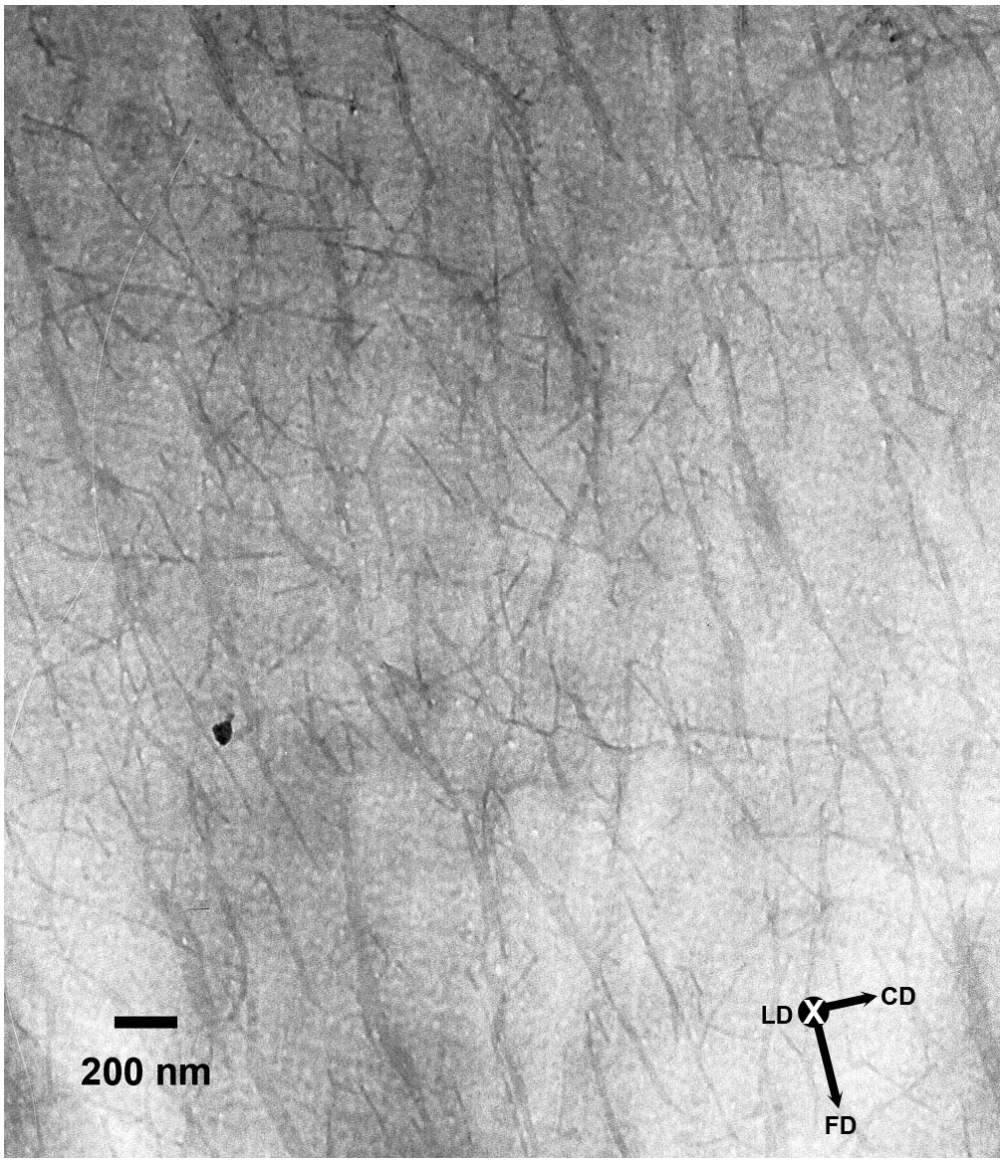

Figure 3.20: Lower-magnification TEM image showing the large-scale orientation of the block copolymer. Because of the large number of viruses on the surface, the underlying block copolymer microstructure is somewhat obscured, but the predominant direction of virus alignment can be seen heading off to the lower right of the micrograph.

3.5 Conclusions

In this chapter it was shown that nickel-loaded PS/P4VP block copolymer is capable of binding both TMV and TNV virions. Nickel ion added in solution is contained in the block copolymer's P4VP microstructure by metal chelation to the pyridine nitrogen. Microphase separation of the PS/P4VP cast from a mixed 91.5 % $CHCl_3$/8 % THF solvent resulted in a cylindrical microstructure with the nickel residing in the P4VP block.

The cylinder long axis of the microstructure was oriented using a hot press and a cooled channel die for quenching, resulting in PS/P4VP cylinders that had a strong anisotropic directional preference. This microstructure, when exposed by microtoming, was seen in the electron microscope to be able to bind both TMV and TNV virions when loaded with nickel.

Without nickel, the binding ability of the surface was no different than that of the Spurr's epoxy used to fix the PS/P4VP for microtoming. The biodetergent Tween was used to test binding because of its known ability to disrupt weak, nonspecific binding in biological systems. In Tween washes of up to 2 hours, TMV remained visible on the surface in increasingly diminished, but still significant, amounts. TMV, because of its size, was seen to cross several cylinders and often formed aggregates with other nearby TMV, although this did not seem to have an affect on the binding ability of the PS/P4VP surface.

It was also seen that when exposed to flowing solutions of TMV, the PS/P4VP-

Ni surface exhibited an ability to retain TMV in a partially aligned state, when the direction of flow coincided with the long axis of the PS/P4VP-Ni cylinders.

Therefore, it is concluded that unlike-charge Coulombic interaction is the dominant mechanism in binding of the negatively charged TMV and TNV to the positively charged PS/P4VP-Ni block copolymer surface. The viability of virus nanopatterning by the PS/P4VP-Ni surface is validated by these results, and it should now be possible to further investigate the binding viruses onto charge-bearing or otherwise functionalized block copolymer surfaces.

Chapter 4

Future Work

There are many opportunities to advance the study of virus and protein nanopatterning by block copolymers beyond this dissertation. It is hoped that the suggestions contained in this section will lead to productive applications of the concepts advanced in this writing.

In analyzing the nanopatterning of hisGFP by the norbornene block copolymer, only fluorescence spectrometry was used to analyze the presence or absence of the protein on the block copolymer surface. Although this is an accurate representation of the presence or absence of surface-bound hisGFP, it is not able to determine the exact location of the binding, nor is it able to determine the orientation of the hisGFP once it has bound to the surface.

Atomic force microscopy (AFM) experiments could resolve the location of the protein on the surface, as could high-resolution scanning electron microscopy (SEM). The film casting would have to be modified, from static-casting to spin-

casting, in order to produce a near-flat copolymer surface that could be read by the AFM tip. Near-field scanning optical microscopy (NFSOM) could be used to locate individual fluorescing hisGFP and this positional data could be correlated to the known sizes of the block copolymer microstructure. NFSOM could also be used to quantify the amount of hisGFP on the surface, allowing for the development of a wash constant of hisGFP from the copolymer surface during Tween detergent washes.

The block copolymer surface, which is capable of binding hisGFP, should be subjected to competition from imidazole, which is normally used in the washing of his-tagged proteins from nickel chelation columns. The purpose of such a competitive wash would be to determine if in fact such a competitive wash would be successful, allowing some understanding of the binding strength of the hisGFP to the copolymer surface. The use of stoichiometric amounts of imidazole would also help quantify the amount of protein washed from the surface. It would also help to determine the re-usability of the surface, a critical concern if this material is to eventually function as part of a device.

A wash constant could also be developed for the system of TMV and TNV on the surface of PS/P4VP-Ni. First and foremost in this effort would be to develop a positive way to determine the presence or absence of TMV and TNV from the surface. One possible way is through the use of picture analyzing software that could identify and count virus particles, such as NIH Image or ImageJ. However,

in certain cases, the "shadow" of a virus on the surface was indeterminate to whether it was a poorly-stained virus or the remnants of virus that was no longer present of the copolymer surface. In this case, AFM would be easily able to distinguish virus rods from proteins on the surface. Also, X-ray photoelectron spectroscopy could be used to detect the presence or absence of the virus by identifying the bonds on the surface characteristic of the virus proteins.

With the ability to easily quantify the amount of virus on the surface, it would be valuable to determine a wash constant that describes the rate of virus removal during Tween washes. This value would allow quantitative analysis between different wash procedures and determination of binding strengths of virus to copolymer.

In the virus-PS/P4VP-Ni system, as in the norbornene-hisGFP system, experiments could be performed to determine the re-usability of the virus binding surface. Long or high concentration Tween washes to remove viruses followed by re-binding and binding population analysis would most likely accomplish this goal.

Flow experiments might be performed that flow TMV perpendicular to the axis of the aligned block copolymer. The purpose of such an experiment would be to see whether PS/P4VP-Ni can align the TMV when the virus rods are not already preferentially aligned to the axis of the block copolymer.

One final possible experiment is the modification of the PS/P4VP-Ni surface

to be more active in the affecting the final orientation of the TMV particle. For example, the PS/P4VP-Ni surface could be chemically modified after film casting to sulfonate the polystyrene. This would result in the post-casting creation of an amphoteric copolymer, with the poly(4-vinylpyrinde) block displaying virus-attractive positive charge from nickel ions, while the newly sulfonated polystyrene block would repel the virus particle with a negative charge.

BIBLIOGRAPHY

[1] Lewandowski, A.T., Small, D.A., Chen, T., Payne, G.F., Bentley, W.E., *Biotechnology and Bioengineering*, **2006**, *93*(6), 1207-1215.

[2] Pederson, J., Lauritzen, C., Madsen, M.T., Dahl, S.W., *Protein Expression and Purification*, **1999**, *15*, 389-400.

[3] Trummer, N., Adanyi, N., Varadi, M., Szendro, I., *Fresenius Journal Of Analytical Chemistry*, **2001**, *371*(1), 21-24.

[4] Yin, T.J., Wei, W.Z., Yang, L., Gao, X.H., Gao, Y.P., *Sensors And Actuators B-Chemical*, **2006**, *117*(1), 286-294.

[5] Wang, Z.J., Yang, Y.H., Li, J.S., Gong, J.L., Shen, G.L., Yu, R.Q., *Talanta*, **2006**, *69*(3), 686-690.

[6] Kwong, P.D., Wyatt, R., Majeed, S., Robinson, J., Sweet, R.W., Sodroski, J., Hendrickson, W.A., *Structure*, **2000**, *8*(12), 1329-1339.

[7] de Oliveira, P.T., Nanci, A., *Biomaterials*, **2004**, *25*(3), 403-413.

[8] Ridet, J.L., Malhotra, S.K., Privat, A., Gage, F.H., *Trends in Neurosciences*, **1997**, *20*(12), 570-577.

[9] Castner, D.G., Ratner, B.D., *Surface Science*, **2002**, *500*(1-3), 28-60.

[10] Image copyrighted by Agilent Technologies, **1998**.

[11] Image copyrighted by Agilent Technologies, **2000 - 2006**.

[12] Seeman, N.C., *Nature*, **2003**, *421*, 427-431.

[13] Braich, S.R., Chelyapov, N., Johnson, C., Rothemund, P.W.K., Aldeman, L, *Science*, **2002**, *296*, 499-502.

[14] Castelvetro, V., De Vita, C., *Advances in Colloid and Interface Science*, **2004**, *108-09*, 167-185.

[15] Kim, K.J., Shahinpoor, M., *Polymer*, **2002**, *43*(3), 797-802.

[16] Allender, C.J., Richardson, C., Woodhouse, B., Heard, C.M., Brain, K.R., *International Journal of Pharmaceuticals*, **2000**, *195*(1-2), 39-43.

[17] Ansell, R.J., Kriz, D., Mosbach, K., *Curent Opinion in Biotechnology*, **1996**, *7*(1), 89-94.

[18] Taboas, J.M., Maddox, R.D., Krebsbach, P.H., Hollister, S.J., *Biomaterials*, **2003**, *24*(1), 181-194.

[19] Lewis, A.L., *Colloids and Surfaces B - Biointerfaces*, **2000**, *18*(3-4), 261-275.

[20] Nakamura, T., Akutagawa, T., Honda, K., Underhill, A.E., Coomber, A.T., Friend, R.H., *Nature*, **1998**, *394*, 159-162.

[21] Holland, N.B., Qiu, Y.X., Ruegsegger, M., Marchant, R.E., *Nature*, **1998**, *392*, 799-801.

[22] Tanev, P.T., Liang, Y., Pinnavaia, T.J., *Journal of the American Chemical Society*, **1997**, *119*(37), 8616-8624.

[23] Tanev, P.T., Pinnavaia, T.J., *Science*, **1996**, *271*, 1267-1269.

[24] Kriz, D., Ramstrom, O., Svensson, A., Mosbach, K., *Analytical Chemistry*, **1995**, *67*(13), 2142-2144.

[25] Bissell, R.A., Cordova, E., Kaifer, A.E., Stoddart, J.F., *Nature*, **1994**, *368*, 834-836.

[26] Dupont-Gillian, C.C., Rouxhet, P.G., *Nano Letters*, **2001**, *1*, 245.

[27] Niederweis, M., Heinz., C., Janik, K., Bossmann, S.H., *Nano Letters*, **2001**, *1*, 169.

[28] Kim, S.R., Abbott, N.L., *Advanced Materials*, **2001**, *13*, 1445.

[29] Demers, L.M., *et al.*, *Angewandte Chemie International Edition*, **2001**, *40*, 3071.

[30] Loidl-Stahlhofen, A., *et al.*, *Advanced Materials*, **2001**, *13*, 1829.

[31] Peterman, M.C., *et al.*, *Artificial Organs*, **2003**, *27*(11), 975-985.

[32] Aghelia, H., Malmstroma, J., Hanarpa, P., Sutherland, D.S., *Materials Science and Engineering: C*, **2006**, *26*(5-7), 911-917.

[33] Flemming, R.G., Murphy, C.J., Abrahams, G.A., Goodman S.L., Nealey, P.F., *Biomaterials*, **1999**, *20*, 573-588.

[34] Leibler, L., *Macromolecules*, **1980**, *13*, 1602-1617.

[35] Aggarwal, S.L., *Polymer*, **1976**, *17*(11), 938-956.

[36] Lodge, T.P., Muthukumar, M., *Journal Of Physical Chemistry*, **1996**, *100*(31), 13275-13292.

[37] Thomas, E.L., Lescanec, R.L., *Philosophical Transactions of the Royal Society of London Series A-Mathematical Physical and Engineering Sciences*, **1994**, *348*(1686), 149-166.

[38] Matsen, M.W., Bates, F.S., *Journal of Polymer Science Part B - Polymer Physics*, **1997**, *35*(6), 945-952.

[39] Schultz, A.R., Flory, P.J., *Journal of the American Chemical Society*, **1952**, *74*(19), 4760-4767.

[40] Schultz, A.R., Flory, P.J., *Journal of the American Chemical Society*, **1953**, *75*(16), 3888-3892.

[41] Cooke, P.R., Smith, J.R.L., *Journal of the Chemistry Society-Perkin Transactions*, **1994**, *1*(14), 1913-1923.

[42] Prause, S., Spange, S., *Journal of Physical Chemistry B*, **2004**, *108*(18), 5734-5741.

[43] Doherty, A.P., Stanley, M.A., Arana, G., Koning, C.E., Brinkhuis, R.H.G., Vos J.G., *Electroanalysis*, **1995**, *7*(4), 333-339.

[44] Read, N., Sachdev, S., *Physical Review Letters*, **1991**, em 66(13), 1773-1776.

[45] Koga, T., Jerome, J.L., Rafailovich, M.H., Sokolov, J.C., Gordon, C., *Journal of Adhesion*, **2005**, *81*(7-8), 751-764.

[46] Clay, R.T., Cohen, R.E., *Supramolecular Science*, **1997**, *4*(1-2), 113-119.

[47] Ciebien, J.F., Clay, R.T., Sohn, B.H., Cohen, R.E., *New Journal of Chemistry*, **1998**, *22*(7), 685-691.

[48] Clay, R.T., Cohen, R.E., *New Journal of Chemistry*, **1998**, *22*(7), 745-748.

[49] Clay, R.T., Cohen, R.E., *Supramolecular Science*, **1995**, *2*(3-4), 183-191.

[50] Teng, Y., Morrison, M.E., Munk, P., Webber, S.E., Prochazka, K., *Macromolecules*, **1998**, *31*(11), 3578-3587.

[51] Roldughin, V.I., Vysotskii, V.V., *Progress in Organic Coatings*, **2000**, *39*(2-4), 81-100.

[52] Nguyen, S.T., Johnson, L.K., Grubbs, R.H., Ziller, J.W., *Journal of the American Chemical Society*, **1992**, *114*(10), 3974-3975.

[53] Novak, B.M., Risse, W., Grubbs, R.H., *Advances in Polymer Science*, **1992**, *102*, 47-72.

[54] Grubbs, R.H., *Journal of Macromolecular Science-Pure and Applied Chemistry*, **1994**, *A31*(11), 1829-1833.

[55] Hafner, A., van der Schaaf, P.A., Muhlebach, A., *Chimia*, **1996**, *50*(4), 131-134.

[56] Ivin, K.J., Kenwright, A.M., Khosravi, E., Hamilton, J.G., *Macromolecular Chemistry and Physics*, **2001**, *202*(18), 3624-3633.

[57] Schrock, R.R., Murdzek, J.S., Bazan, G.C., Robbins, J., Dimare, M., ORegan, M., *Journal of the American Chemical Society*, **1990**, *112*, 3875.

[58] Schwab, P., Grubbs, R.H., Ziller, J.W., *Journal of the American Chemical Society*, **1996**, *118*, 100.

[59] Slugovc, C., Perner, B., Stelzer, F., Mereiter, K., *Organometallics*, **2004**, *23*(15), 3622-3626.

[60] Casey, J.L., Keep, P.A., Chester, K.A., Robson, L., Hawkins, R.E., Begent, R.H.J., *Journal of Immunological Methods*, **1995**, *179*(1), 105-116.

[61] Kronina, V.V., Wirth, H.J., Hearn, M.T.W., *Journal of Chromatography A.*, **1999**, *852*(1), 261-272.

[62] Kang, E.T., Tan, E.L., Kato, K., Uyama, Y., Ikada, Y., *Macromolecules*, **1996**, *29*, 6872-6879.

[63] Cummins, C.C., Beachy, M.D., Schrock, R.R., Vale, M.G., Sankaran, V., Cohen, R.E., *Chemistry of Materials*, **1991**, *3*, 1153-1163.

[64] Voros, J., Blattler, T., Textor, M., *MRS Bulletin*, **2005**, *30(3)*, 202-206.

[65] Kumar, N., Hahm, J., *Langmuir*, **2005**, *21*, 6652-6655.

[66] Millot, M.C., Herve, F., Sebille, B., *Journal of Chromatography B-Biomedical Applications*, **1995**, *664(1)*, 55-67.

[67] Li, S., Dass, C. *Analytical Biochemistry*, **1999**, *270*, 9-14.

[68] Porath, J., Olin, B., *Biochemistry*, **1983**, *22(7)*, 1621-1630.

[69] Sulkowski, E., *Trends in Biotechnology*, **1985**, *3*, 1-12.

[70] Porath, J., Carlsson, J., Olsson, I., Belfrage, G., *Nature*, **1975**, *258(5536)*, 598-599.

[71] Chalfie, M., *Photochemistry and Photobiology* **1995**, *62(4)*, 651-656.

[72] Alberts, B., Bray, D., Lewis, J., Raff, M., Roberts, K., Watson, J.D., *Molecular Biology of the Cell, Third Edition* **1994**, *30(3)*, 274-287.

[73] Fauci, A.S., *Clinical Infectious Diseases*, **2001**, *32*, 675-685.

[74] Morens, D.M., Folkers G.K., Fauci A.S., *Nature*, **2004**, *430*, 242-249.

[75] Pimentel D. *et al.*, *Agriculture, Ecosystems and Environment*, **2001**, *84*, 120.

[76] Burdon, J.J., Thrall, P.H., Ericson, L., *Annual Reveiw of Phytopatholgy*, **2006**, *44*, 1939.

[77] Oda, Y., *te al.*, *Journal Molecular Biology*, **2000**, *300*, 153-169.

[78] TEM image copyrighted by Rothamsted Research, Harpenden, Hertfordshire, United Kingdom, AL5 2JQ, **1994**.

[79] Fraden, S., Maret, G., Caspar D.L.D., *Physical Review E*, **1993**, *48*(4), 2816-2838.

[80] Reichel, C., Beachy, R.N., *Proceedings of the National Academy of Sciences*, **1998**, *95*(19), 11169-11174.

[81] Whitham, S., McCormick, S., Baker, S., *Proceedings of the National Academy of Sciences*, **1996**, *93*(16), 8776-8781.

[82] Hwang, D., Roberts, I.M., Wilson, T.M.A., *Proceedings of the National Academy of Sciences*, **1994**, *91*, 9067-9071.

[83] Gooding, G.V., Hebert, T.T., *Phytopathology*, **1967**, *57*, 1285-1286.

[84] Tween 20 (Product Number P5927), available from Sigma-Aldrich, **2006**.

[85] Flemming, R.G., Murphy, C.J., Abrahams, G.A., Goodman S.L., Nealey, P.F., *Biomaterials*, **1999**, *20*, 573-588.